

# Numerical Construction of Elliptic Lower-Dimensional Quasi-Periodic Solutions with a Priori Bound

Mingwei Fu<sup>1</sup> and Bin Shi\*<sup>2,3</sup>

<sup>1</sup>School of Mathematical Sciences, University of Chinese Academy of Sciences, Beijing 100049, China

<sup>2</sup>Center for Mathematics and Interdisciplinary Sciences, Fudan University, Shanghai 200433, China

<sup>3</sup>Shanghai Institute for Mathematics and Interdisciplinary Sciences (SIMIS), Shanghai 200433, China

May 5, 2026

## Abstract

A numerical framework for constructing full-dimensional quasi-periodic solutions in nearly integrable systems was recently developed by [Fu and Shi \[2026\]](#). Based on an alternating scheme, this approach effectively overcomes the secular drift in angle variables, a fundamental limitation of classical symplectic integrators. However, in many applications, such as the restricted three-body problem, lower-dimensional quasi-periodic solutions hold greater significance. The construction of these solutions is considerably more challenging due to the presence of normal frequencies, which give rise to intricate resonance phenomena. Beyond the standard subspace resonance requirements, one must also account for the first and second Melnikov conditions to eliminate small divisors. In this study, we extend the proposed alternating numerical scheme to compute the elliptic lower-dimensional quasi-periodic solutions. Numerical experiments are presented for the Hénon-Heiles model in galaxy scale and the Fermi–Pasta–Ulam (FPU) model in quantum scale, demonstrating the effectiveness of the proposed method. Furthermore, we emphasize that the perturbation Hamiltonian is not merely a polynomial with real coefficients but is a general real-valued function. As a result, the associated perturbation operator exhibits Gevrey-type decay without possessing a Hankel-like structure. Meanwhile, we further simplify the multi-scale analysis by exploiting the resolvent identity, showing that the global inverse can be expressed linearly in terms of local inverses via the gluing procedure. This representation reveals a regime-dependent interaction structure: weak interactions dominate at short range, while strong interactions emerge at long range. This balance ensures that the Gevrey decay of the inverse remains uniformly controlled. Moreover, within this linear representation, the inversion conditions provide a clearer characterization of the associated localization properties.

## 1 Introduction

Nearly integrable systems constitute a fundamental class of Hamiltonian dynamics, serving as a bridge between perfectly predictable, “solvable” dynamics and the complex, chaotic phenomena

---

\*Corresponding author: [binshi@fudan.edu.cn](mailto:binshi@fudan.edu.cn)

observed in nature. They arise across a wide range of physical scales, from the macroscopic long-time stability of planetary orbits in our solar system to the microscopic vibrations of atoms in crystalline lattices. In action-angle coordinates, such systems are described by a Hamiltonian of the form:

$$H(I, \theta) = H_0(I) + \varepsilon H_1(I, \theta),$$

where  $H_0(I)$  is the integrable component and  $\varepsilon H_1(I, \theta)$  is a small nonlinear perturbation with  $0 < \varepsilon \ll 1$ . The phase space is equipped with the standard symplectic form  $\varpi = dI \wedge d\theta$ .

In the absence of perturbation ( $\varepsilon = 0$ ), the dynamics are governed exclusively by  $H_0$ . The resulting motion is explicitly given by:

$$I(t) = I_0, \quad \theta(t) = \theta_0 + \omega(I_0)t, \quad (1.1)$$

where the frequency satisfies  $\omega(I_0) = \nabla H_0(I_0)$ . As a result, the trajectories are confined to  $n$ -dimensional invariant tori in phase space, exhibiting perfectly quasi-periodic behavior. To study the effect of the perturbations, we consider the dynamics in a neighborhood of the unperturbed torus  $\{I_0\} \times \mathbb{T}^n$ . By introducing the shifted action variable  $J = I - I_0$ , we translate this torus to  $\{0\} \times \mathbb{T}^n$ . A Taylor expansion of  $H_0(I)$  about  $I_0$  allows us to reformulate the Hamiltonian as:

$$H(J, \theta; I_0) = \langle \omega(I_0), J \rangle + \varepsilon H_1(J, \theta; I_0), \quad (1.2)$$

where the constant term  $H_0(I_0)$  is omitted, as it does not affect the equations of motion. Note that the redefined perturbation term  $H_1$  incorporates both the original perturbation and the higher-order terms (second-order and above) arising from the expansion of  $H_0$ . A rigorous derivation can be found in Pöschel [2001].

We restrict our attention to initial actions  $I_0$  in a bounded domain  $D_n \subseteq \mathbb{R}^n$ , which necessitates an analysis of the frequency map  $\omega : D_n \rightarrow \Omega_n \subseteq \mathbb{R}^n$ . If this map is a diffeomorphism, the Hamiltonian (1.2) can be reparameterized directly by the frequency  $\omega \in \Omega_n$ :

$$H(J, \theta; \omega) = \langle \omega, J \rangle + \varepsilon H_1(J, \theta; \omega). \quad (1.3)$$

The validity of this reparameterization is ensured by the isoenergetic non-degeneracy condition. Specifically, if the following determinant remains non-zero for all  $I_0 \in D_n$ :

$$\det \begin{pmatrix} \nabla^2 H_0 & \nabla H_0 \\ (\nabla H_0)^\top & 0 \end{pmatrix} \neq 0,$$

then the frequency map  $\omega : I_0 \mapsto \omega(I_0)$  is guaranteed to be a diffeomorphism (see e.g. Arnold [2013]). Throughout this work, we assume that all components of the frequency  $\omega \in \Omega_n$  are non-zero, i.e.,  $\omega_j \neq 0$  for  $j = 1, \dots, n$ , and that  $H_1$  is at least quadratic in  $J$ . If  $H_1$  contained linear terms in  $J$ , it would contribute to the effective frequency, necessitating a frequency drift correction to preserve the resonance conditions.

## 1.1 Lower-dimensional tori

We now consider solutions of the nearly integrable system (1.3), with particular emphasis on perturbed trajectories near the unperturbed  $n$ -torus  $\{0\} \times \mathbb{T}^n$ . To characterize the domain  $D_n$ , let  $\mathcal{H}_j$  denote the  $j$ -th coordinate hyperplane

$$\mathcal{H}_j = \{I_0 \in \mathbb{R}^n | I_{0,j} = 0\}$$

for  $j = 1, \dots, n$ . When the domain  $D_n$  is set apart from these hyperplanes, i.e.,  $D_n \cap \mathcal{H}_j = \emptyset$  for all  $j$ , then the system operates in the regime of full-dimensional tori. In this setting, the classical KAM theorem, pioneered by Kolmogorov [1954], Arnold [1963] and Moser [1962], serves as a fundamental landmark, which asserts that most invariant tori persist under sufficiently small perturbations, provided that they remain away from the resonant set:

$$\langle k, \omega \rangle = 0, \quad (1.4)$$

for all non-zero integer vectors  $k \in \mathbb{Z}^n \setminus \{0\}$ .

In many physical systems, however, some components of the initial action  $I_0$  may vanish, i.e.,  $D_n \cap \mathcal{H}_j \neq \emptyset$  for some  $j$ , as noted by Moser [1966]. A classic example is the restricted three-body problem (e.g., the Sun-Earth-Moon system), where one action variable, associated with the eccentricity of the primary (e.g., the Sun), vanishes in the integrable limit. In such cases, we may assume without loss of generality that the first  $m$  components are non-zero while the remaining  $n - m$  components vanish:  $I_0 \in D_m \times \{0\} \subseteq \mathbb{R}^m \times \mathbb{R}^{n-m}$ . The frequency then decomposes into tangential and normal components,  $\omega = (\omega_T, \omega_N)$ . The Hamiltonian (1.3) can then be rewritten as

$$H(J, \theta, z, \bar{z}; \omega) = \langle \omega_T, J \rangle + \langle \omega_N(\omega_T) z, \bar{z} \rangle + \varepsilon H_1(J, \theta; z, \bar{z}; \omega_T). \quad (1.5)$$

where  $\omega_T(I_0) = \nabla H_0(I_0)$  satisfies the isoenergetic non-degeneracy condition. The phase space carries the symplectic form  $\varpi = dJ \wedge d\theta + idz \wedge d\bar{z}$ . Since only  $m < n$  components are non-zero, the associated invariant manifolds are  $m$ -dimensional tori embedded in  $2n$ -dimensional space, referred to as lower-dimensional tori. We focus on the behavior of trajectories near the unperturbed torus  $\{0\} \times \mathbb{T}^m \times \{0\} \times \{0\}$ . When the normal frequencies are real, i.e.,  $\omega_N \in \mathbb{R}^{n-m}$ , these lower-dimensional invariant tori are called elliptic. In this case, the resonant structure becomes more intricate. As first noted by Melnikov [1965, 1968], in addition to the standard resonance condition (1.4) for all  $k \in \mathbb{Z}^m \setminus \{0\}$ , one must also consider the first Melnikov resonant condition:

$$\langle k, \omega_T \rangle - \omega_j = 0, \quad (1.6)$$

for all  $k \in \mathbb{Z}^m$  and  $j = m + 1, \dots, n$ , as well as the second Melnikov resonant condition:

$$\begin{cases} \langle k, \omega_T \rangle - \omega_{j_1} + \omega_{j_2} = 0, & (1.7a) \\ \langle k, \omega_T \rangle - \omega_{j_1} - \omega_{j_2} = 0, & (1.7b) \end{cases}$$

for all  $k \in \mathbb{Z}^m$  and  $j_1, j_2 = m + 1, \dots, n$ . The KAM theorems established by Eliasson [1988] and Pöschel [1989] show that most elliptic lower-dimensional invariant tori persist under sufficiently small perturbations, provided that these resonant conditions are avoided. In contrast, if some normal frequencies are complex, i.e.,  $\text{Im}(\omega_j) \neq 0$  for some  $j > m$ , the corresponding lower-dimensional tori are termed hyperbolic, as first discussed by Moser [1967]. Unlike their elliptic counterparts, these hyperbolic tori are inherently unstable. Transversal intersections of their stable and unstable manifolds generate chains of homoclinic or heteroclinic orbits, which give rise to Arnold diffusion [Arnold, 1964], a phenomenon where trajectories undergo a slow, long-term drift in action variables across the phase space.

## 1.2 Numerical scheme and iterative framework

Unlike traditional normal form techniques in KAM theory, which employ successive symplectic transformations to separate perturbed dynamics from integrable motion, the Craig-Wayne-Bourgain

(CWB) scheme adopts a more direct strategy. Originally established by Bourgain [1997, 2005] for constructing elliptic lower-dimensional quasi-periodic solutions, this method avoids the explicit decomposition into integrable and perturbative components. Instead, it works directly with the Hamiltonian:

$$H(I, \theta; \omega) = \langle \omega, I \rangle + \varepsilon H_1(I, \theta; \omega_T), \quad (1.8)$$

where the initial action is confined to a lower-dimensional subspace:  $I_0 \in D_m \times \{0\} \subseteq \mathbb{R}^m \times \mathbb{R}^{n-m}$ . Traditional numerical simulations typically rely on symplectic integrators [Feng, 1995, Hairer et al., 2006, Gauckler et al., 2018]. While these methods are highly effective at preserving underlying geometric structures, they suffer from an inherent limitation: the accumulation of phase errors, which leads to secular drift in the angle variables. This drift significantly degrades the long-time accuracy of quasi-periodic trajectories. In this paper, we generalize the numerical framework introduced by Fu and Shi [2026] to construct elliptic lower-dimensional quasi-periodic solutions with any prescribed level of accuracy, while effectively mitigating the drift issues that arise in standard time-integration methods.

By applying the complex canonical transformation,  $z_j = \sqrt{I_j} e^{i\theta_j}$  for  $j = 1, \dots, n$ , the Hamiltonian (1.8) is rewritten as

$$H(z, \bar{z}) = \langle \omega \odot z, \bar{z} \rangle + \varepsilon H_1(z, \bar{z}), \quad (1.9)$$

where  $\odot$  denotes componentwise multiplication. For simplicity, we omit the explicit dependence on the tangential frequencies  $\omega_T$  within  $H_1$ , since all relevant properties of the perturbation hold uniformly across the domain with respect to  $\omega_T$ ; this convention is adopted throughout the remainder of the paper. Under the symplectic form  $dz \wedge d\bar{z} = -idI \wedge d\theta$ , the Hamilton's equations of motion are expressed as:

$$\dot{z} = i\omega \odot z + i\varepsilon \frac{\partial H_1}{\partial \bar{z}}. \quad (1.10)$$

We now transform the Hamiltonian system (1.10) to an algebraic system available for numerical computation. Since the procedure closely follows Fu and Shi [2026], we only provide a brief outline here. We seek quasi-periodic solutions of the form

$$z(\omega'_T t) = \sum_{k \in \mathbb{Z}^m} \hat{z}(k) e^{i\langle k, \omega'_T \rangle t}, \quad (1.11)$$

where  $\hat{z}(k) \in \mathbb{R}^n$  are real Fourier coefficients, which constitute a key feature of the present approach. Substituting this ansatz (1.11) into the Hamiltonian system (1.10), we derive the following algebraic system as

$$-\langle k, \omega'_T \rangle \hat{z} + \omega \odot \hat{z} + \varepsilon \hat{X} = 0, \quad (1.12)$$

where  $\hat{X} = \{\hat{X}(k)\}_{k \in \mathbb{Z}^m}$  is the vector of Fourier coefficients corresponding to the perturbation  $X = \partial H_1 / \partial \bar{z}$ . We here focus on the elliptic lower-dimensional quasi-periodic solutions, with initial action  $I_0 = a = (a_1, \dots, a_m, 0, \dots, 0)$ . Let  $\mathcal{M} = \{1, \dots, m\}$ , and define the set of resonant indices

$$\mathcal{S} = \{(j, e_j) | j = 1, \dots, m\}, \quad (1.13)$$

where  $e_j \in \mathbb{Z}^m$  is the standard basis vector. Accordingly, we decompose the Fourier coefficients and the vector field into resonant and non-resonant parts:  $\hat{z} = (\hat{z}_q, \hat{z}_p)^\top$  and  $\hat{X} = (\hat{X}_q, \hat{X}_p)^\top$ , where the resonant part is given by  $\hat{z}_q = (\hat{z}_1(e_1), \dots, \hat{z}_m(e_m))$  and  $\hat{X}_q = (\hat{X}_1(e_1), \dots, \hat{X}_m(e_m))$ . For resonant

indices  $(j, k) \in \mathcal{S}$ , the coefficients are fixed as  $\hat{z}_j(e_j) = a_j$ , so that  $\hat{z}_q = a$ . The tangential frequencies are then determined by the  $Q$ -equation:

$$(-\omega'_T + \omega_T) \odot a + \varepsilon \hat{X}_q = 0. \quad (1.14)$$

For non-resonant indices  $(j, k) \notin \mathcal{S}$ , the non-resonant coefficients  $\hat{z}_p$  are obtained from the  $P$ -equation:

$$-\langle k, \omega'_T \rangle \hat{z}_p + \omega \odot \hat{z}_p + \varepsilon \hat{X}_p = 0. \quad (1.15)$$

Since the  $P$ -equation (1.15) constitutes an infinite-dimensional nonlinear algebraic equation, we employ a dimension-enlarged Newton scheme for its numerical solution. To this end, we define the nonlinear operator  $F$ , acting on the non-resonant Fourier coefficients  $\hat{z}_p$ , as:

$$F(\omega'_T, \hat{z}_p; a, \omega) = -\langle k, \omega'_T \rangle \hat{z}_p + \omega \odot \hat{z}_p + \varepsilon \hat{X}_p(\hat{z}_p; a). \quad (1.16)$$

The associated linearized (tangent) operator takes the form  $T = D + \varepsilon S$ , where  $D$  is a diagonal operator and  $S$  is the Jacobian arising from the nonlinear perturbation. More precisely,

$$D = \text{diag}(-\langle k, \omega'_T \rangle E_n + \omega), \quad \text{and} \quad S = \frac{\partial \hat{X}_p(\omega, \hat{z}_p; a)}{\partial \hat{z}_p}, \quad (1.17)$$

where  $E_n$  denotes the identity matrix on  $\mathbb{R}^n$ . In the case of lower-dimensional quasi-periodic solutions ( $m < n$ ), the integer combinations  $\langle k, \omega'_T \rangle$  involve fewer independent variables. As a consequence, the diagonal entries of  $D$  exhibit higher multiplicity, meaning that multiple Fourier modes share the same tangential frequency components. This leads to a ‘‘clustering’’ of eigenvalues and a significant reduction in the prevalence of small divisors. In this sense, lower-dimensional quasi-periodic solutions are generally more accessible than their full-dimensional counterparts.

Let  $M = M(\varepsilon)$  be a positive integer, whose explicit definition is given in (3.4), and define the truncation scale by  $N_r := M^r$ . Based on the  $Q$ -equation (1.14) and the  $P$ -equation (1.15), we propose the following iterative scheme to update the frequency and the non-resonant coefficients from the  $r$ -th to the  $(r + 1)$ -th step:

$$\begin{cases} \omega_T^{(r+1)} = \omega_T + \varepsilon \hat{X}_q(\hat{z}_p^{(r)}; a) \odot a^{-1}, & (1.18a) \\ \hat{z}_p^{(r+1)} = \hat{z}_p^{(r)} - \left[ (T + \varepsilon B)_{N_{r+1}}^{-1} \left( \hat{z}_p^{(r)}, \omega_T^{(r+1)}; a \right) \right] F \left( \hat{z}_p^{(r)}, \omega_T^{(r+1)}; a, \omega \right). & (1.18b) \end{cases}$$

where  $a^{-1} = (a_1^{-1}, \dots, a_m^{-1})$ . The operator  $B$  is introduced to ensure the convergence of the iteration which is given by

$$B = -\frac{1}{e} \left( \frac{\partial \langle k, \hat{X}_q \rangle}{\partial \hat{z}_p} \right) \hat{z}_p^\top. \quad (1.19)$$

The restricted operator is defined as  $(T + \varepsilon B)_N = P_N(T + \varepsilon B)P_N$ , where  $P_N$  is the projection operator given by

$$(P_N \hat{z})(k) := \begin{cases} \hat{z}(k), & \text{if } k \in \Lambda_N, \\ 0, & \text{if } k \notin \Lambda_N, \end{cases}$$

and the truncation domain, or box lattice, is defined as:

$$\Lambda_N := \{k \in \mathbb{Z}^m \mid |k|_\infty \leq N\}. \quad (1.20)$$

Throughout this paper, unless otherwise specified,  $|\cdot|$  and  $|\cdot|_\infty$  denote the  $\ell_1$ -norm and the  $\ell_\infty$ -norm, respectively, on  $\mathbb{Z}^m$  or  $\mathbb{R}^m$ .

### 1.3 The main theorem: A priori bound

In this section, we establish an a priori bound for the alternating numerical procedure (1.18). For the Fourier coefficients  $\hat{z} = \{\hat{z}(k)\}_{k \in \mathbb{Z}^m}$ , we denote the standard  $\ell_2$ -norm as:

$$\|\hat{z}\|_2 = \left( \sum_{k \in \mathbb{Z}^m} \|\hat{z}(k)\|_2^2 \right)^{\frac{1}{2}}.$$

Given that the Fourier vector  $\hat{z}$  is continuously differentiable with respect to the tangential frequency  $\omega_T$ , we introduce the normed vector space

$$\mathcal{H}(\mathbb{Z}^m) = \left\{ \hat{z} = \{\hat{z}(k)\}_{k \in \mathbb{Z}^m} \mid \hat{z}(k) \in \mathbb{R}^n, \|\hat{z}\| = \|\hat{z}\|_2 + \|\partial_{\omega_T} \hat{z}\|_2 < \infty \right\}. \quad (1.21)$$

To characterize the regularity of solutions, we define the Gevrey decay set:

$$\mathcal{K}(s) = \left\{ \hat{z} \in \mathcal{H}(\mathbb{Z}^m) \mid \sup_{k \in \mathbb{Z}^m} (\|\hat{z}(k)\| \exp\{|k|^s\}) \leq 1 \right\}, \quad (1.22)$$

where the sub-exponential decay of these Fourier coefficients plays a key role in preserving the regularity of the iterative scheme.

**Theorem 1.1** (Convergence and A Priori Bound). Let  $\Omega \subseteq \mathbb{R}^m$  be a bounded domain, and let  $\tau > m - 1$  be fixed. There exists a critical threshold  $\varepsilon_0 = \varepsilon_0(H_1, \Omega, a) > 0$  such that for any  $0 < \varepsilon \leq \varepsilon_0$ , the following properties hold:

1. **Measure of resonance:** There exist constants  $\kappa = \kappa(n, m, \tau, \Omega) > 0$  and  $\delta = \delta(\varepsilon) > 0$ , with  $\delta \rightarrow 0$  as  $\varepsilon \rightarrow 0$ , such that the excluded set of “bad” frequencies  $\Omega^*$  satisfies  $\text{mes}(\Omega^*) \leq \kappa + \delta$ .
2. **Iterative sequence:** For any initial pair  $\omega_T^{(0)} \in \Omega \setminus \Omega^*$  and  $\hat{z}_p^{(0)} = 0$ , the alternating numerical procedure (1.18) generates a sequence of iterates  $\{(\omega_T^{(r)}, \hat{z}_p^{(r)})\}_{r=0}^\infty$ .
3. **Convergence:** There exists a Gevrey exponent  $s = s(\varepsilon)$  such that this sequence remains within the product space  $(\Omega \setminus \Omega^*) \times \mathcal{K}(s)$  and converges to the exact solution pair  $(\omega_T^*, \hat{z}_p^*)$ .
4. **A priori bound:** There exists a constant  $M = M(\varepsilon)$  such that the convergence is characterized by the following super-exponential error bounds:

$$\left\{ \|\hat{z}^{(r)} - \hat{z}^*\| \leq \exp \left\{ -\frac{3}{2}(M^s)^r \right\}, \right. \quad (1.23a)$$

$$\left. \left| \omega_T^{(r)} - \omega_T^* \right| \leq \exp \left\{ -\frac{3}{2}(M^s)^r \right\}. \right. \quad (1.23b)$$

Furthermore, for any  $t \in [0, M^r]$ , the approximate solution  $z^{(r)}(t)$  satisfies the error bound:

$$\|z^{(r)}(t) - z^*(t)\| \leq \exp \{-(M^s)^r\}. \quad (1.24)$$

This implies that as  $r \rightarrow \infty$ , the numerical solution  $z^{(r)}(t)$  converges to the exact quasi-periodic solution  $z^*(t)$  for any  $t \geq 0$ .

Theorem 1.1 remains valid under the stated analytic assumptions. The complete proof is finalized in Section 5, synthesizing the implementation framework established in Section 3 and the multi-scale analysis presented in Section 4.

## 1.4 Organization of the paper

The remainder of this paper is organized as follows. Section 2 establishes uniform properties of the associated vectors and operators within the Gevrey decay class, which serve as the foundation for the subsequent analysis. Section 3 formulates the implementation conditions and provides the corresponding proofs using inductive arguments. Section 4 derives the inversion and localization conditions for the tangent operator restricted to outer boxes via a multi-scale analysis, built upon inductive bases for two types of small-scale cases. Section 5 establishes the iterative lemma and provides the proof of the main convergence results. Section 6 presents numerical experiments on both the macroscopic Hénon–Heiles model and the microscopic Fermi–Pasta–Ulam (FPU) model. Finally, Section 7 concludes the paper and outlines directions for future research.

## 2 Uniform properties within the Gevrey decay set

In this section, we establish uniform decay and boundedness properties for the associated vectors and operators within the Gevrey decay set  $\mathcal{K}(s)$ . Let  $\mathbb{T}^m = [0, 2\pi]^m$  denote the  $m$ -dimensional torus. For any  $k \in \mathbb{Z}^m$ , the component of the vector field  $\hat{X}$  is given by

$$\hat{X}(k) = \frac{1}{(2\pi)^m} \int_{\mathbb{T}^m} \frac{\partial H_1}{\partial \bar{z}} e^{-i\langle k, \theta \rangle} d\theta. \quad (2.1)$$

Since  $H_1$  is a polynomial with real coefficients,  $\hat{X}(k)$  is real-valued. Furthermore, because the perturbation  $H_1$  is real, the following symmetric relation holds:

$$\frac{1}{(2\pi)^m} \int_{\mathbb{T}^m} \frac{\partial H_1}{\partial \bar{z}} e^{-i\langle k, \theta \rangle} d\theta = \frac{1}{(2\pi)^m} \int_{\mathbb{T}^m} \frac{\partial H_1}{\partial z} e^{i\langle k, \theta \rangle} d\theta. \quad (2.2)$$

We now establish the following property for the vector field  $\hat{X} = (\hat{X}_q, \hat{X}_p)^\top$  (see Section A.2 for a formal proof).

**Proposition 2.1.** Suppose  $\hat{z} \in \mathcal{K}(s)$ . Then there exist constants  $\gamma_1, \gamma_2 > 0$ , depending on  $H_1$  and  $s$ , such that the vector field  $\hat{X}$  satisfies

$$\begin{cases} \sup_{k \in \mathbb{Z}^m} \left( \|\hat{X}(k)\| \exp\{|k|^s\} \right) \leq \gamma_1, & (2.3a) \\ \max \{ \|\hat{X}_q\|, \|\hat{X}_p\| \} \leq \|\hat{X}\| \leq \gamma_2. & (2.3b) \end{cases}$$

Next, we analyze the tangent operator  $\partial \hat{X} / \partial \hat{z}_p = (\partial \hat{X}_q / \partial \hat{z}_p, \partial \hat{X}_p / \partial \hat{z}_p)^\top$ . Recalling the tangent operator defined in (1.17), it follows that  $S = \partial \hat{X}_p / \partial \hat{z}_p$ . For any two resonant indices  $k, k' \notin \mathcal{S}$ , we utilize (2.2) to derive its component as

$$S(k, k') = S(k - k') = \frac{2}{(2\pi)^m} \int_{\mathbb{T}^m} \frac{\partial^2 H_1}{\partial z \partial \bar{z}} \cos(\langle k - k', \theta \rangle) d\theta.$$

The tangent operator satisfies the following property (see Section A.3 for a formal proof).

**Proposition 2.2.** Suppose  $\hat{z} \in \mathcal{K}(s)$ . Then there exist constants  $\gamma_3, \gamma_4 > 0$ , depending on  $H_1$  and  $s$ , such that the tangent operator  $S$  is symmetric and satisfies:

$$\left\{ \sup_{k, k' \notin \mathcal{S}} (\|S(k, k')\| \exp\{|k - k'|^s\}) \leq \gamma_3, \right. \quad (2.4a)$$

$$\left. \max \left\{ \left\| \frac{\partial \hat{X}_q}{\partial \hat{z}_p} \right\|, \|S\| \right\} \leq \left\| \frac{\partial \hat{X}}{\partial \hat{z}_p} \right\| \leq \gamma_4. \right. \quad (2.4b)$$

To facilitate the iteration lemma (Theorem 5.2), we also require estimates for the second derivative of the vector field  $\hat{X}$ , as stated below (see Section A.4 for the proof).

**Proposition 2.3.** Suppose  $\hat{z} \in \mathcal{K}(s)$ , and assume further that  $\text{supp } \hat{z} \subseteq \Lambda_N$ . Then there exists a constant  $\gamma_5 = \gamma_5(H_1, s, m)$  such that

$$\max \left\{ \left\| \frac{\partial^2 \hat{X}_q}{\partial \hat{z}_p^2} \right\|, \left\| \frac{\partial S}{\partial \hat{z}_p} \right\| \right\} \leq \left\| \frac{\partial^2 \hat{X}}{\partial \hat{z}_p^2} \right\| \leq \gamma_5 (2N + 1)^{\frac{m}{2}}. \quad (2.5)$$

In the numerical scheme, we introduce the frequency iteration (1.18). To control the associated error, we define an additional operator  $B$ , whose properties are summarized below (see Section A.5 for the proof).

**Proposition 2.4.** Suppose  $\hat{z} \in \mathcal{K}(s)$ . Then there exist constants  $\gamma_6, \gamma_7 > 0$ , depending on  $H_1$  and  $s$ , such that the operator  $B$  satisfies:

$$\left\{ \sup_{k, k' \notin \mathcal{S}} (\|B(k, k')\| \exp\{|k|^s + |k'|^s\}) \leq \gamma_6, \right. \quad (2.6a)$$

$$\left. \|B\| \leq \gamma_7. \right. \quad (2.6b)$$

Let  $\gamma = \max_{1 \leq j \leq 7} \gamma_j$ , where each  $\gamma_j$  depends on the perturbation  $H_1$ . By appropriately scaling  $H_1$ , or equivalently, by choosing  $\varepsilon$  sufficiently small, we may assume without loss of generality that  $\gamma \leq 1/(2e) < 1/2$ . Utilizing the boundedness of the vector field  $\hat{X}_q$  and its tangent operator from Theorem 2.1 and Theorem 2.2, we can establish the following result concerning the tangential frequency drift.

**Proposition 2.5.** Suppose  $\hat{z} \in \mathcal{K}(s)$ . Then the tangential frequency drift determined by the  $Q$ -equation (1.14) satisfies:

$$|\omega'_T - \omega_T| \leq \varepsilon, \quad (2.7)$$

and the Jacobian of the tangential frequency map satisfies:

$$1 - \varepsilon \leq \left\| \frac{\partial \omega'_T}{\partial \omega_T} \right\|_2 \leq 1 + \varepsilon. \quad (2.8)$$

Theorem 2.5 ensures that the mapping between the drifted tangential frequency  $\omega'_T$  and the original tangential frequency  $\omega_T$  is a diffeomorphism.

### 3 Implementation conditions

The heart of the alternating numerical scheme (1.18) hinges on updating the non-resonant vector via the dimension-enlarged Newton scheme (1.18b). To overcome the small-divisor problem, we must rigorously control the inverse of the truncated matrix  $(T + \varepsilon B)_N$  as the dimension grows. To this end, we introduce a scale-dependent threshold parameter:

$$\varepsilon_N := \exp \left\{ -(\log N)^{15} \right\}. \quad (3.1)$$

We formulate the following implementation conditions to ensure the convergence of the alternating numerical scheme.

**Condition 3.1** (Implementation Conditions). The truncated linearized operator  $(T + \varepsilon B)_N$  is required to satisfy the following two conditions:

- (1) **Inversion condition:** The operator norm of the inverse is bounded by the reciprocal of the threshold parameter:

$$\|(T + \varepsilon B)_N^{-1}\|_2 \leq \frac{1}{\varepsilon_N}. \quad (3.2)$$

- (2) **Localization condition:** For sufficiently large spatial separations within the lattice  $\Lambda_N$ , specifically when  $|k - k'| \geq N^{\frac{1}{2}}$ , the entries of the inverse matrix must exhibit Gevrey-type decay:

$$|(T + \varepsilon B)_N^{-1}(k, k')| \leq \exp \left\{ -\frac{|k - k'|^s}{2} \right\}. \quad (3.3)$$

These implementation conditions are satisfied by systematically excluding “bad” frequencies. To handle the restricted operators, we distinguish between small and large scales using the threshold  $M$  dictated by the perturbation intensity  $\varepsilon$ :

$$M = \exp \left\{ \left( \log \frac{1}{\varepsilon} \right)^{\frac{1}{20}} \right\}. \quad (3.4)$$

The scale  $N$  is subsequently divided into two distinct regimes: the small-scale regime  $M_0 \leq N \leq M$  and the large-scale regime  $N > M$ , where the initial scale is defined as  $M_0 = \exp \left\{ (\log M)^{\frac{1}{20}} \right\}$ . For notational simplicity, we denote the linearized operator as  $L := T + \varepsilon B$  throughout the remainder of the paper.

#### 3.1 Nearly-resonant sets

We first consider the small-scale regime  $M_0 \leq N \leq M$ . To guarantee the invertibility of the restricted operator, we must exclude the frequencies that trigger resonance. In the case of full-dimensional quasi-periodic solutions, nearly-resonant sets involve the entire frequency  $\omega$ . However, in the lower-dimensional setting, only the tangent frequency  $\omega_T$  is relevant. Accordingly, we define the following nearly-resonant sets in the tangent frequency space, corresponding to the resonance conditions outlined in Section 1.1:

- **Tangent nearly-resonant sets:** Corresponding to the resonance condition (1.4), we define:

$$\Omega_{0,M}^\tau = \bigcup_{k \in \Lambda_{2M} \setminus \{0\}} \left\{ \omega_T \in \Omega \mid |\langle k, \omega_T \rangle| < \frac{1}{|k|^\tau} \right\}. \quad (3.5)$$

- **Single-mode nearly-resonant sets:** Corresponding to the first Melnikov condition (1.6), we define

$$\Omega_{1,M}^\tau = \bigcup_{k \in \Lambda_{2M}} \bigcup_{j=m+1}^n \left\{ \omega_T \in \Omega \mid |\langle k, \omega_T \rangle - \omega_j| < \frac{1}{(|k|+1)^\tau} \right\}. \quad (3.6)$$

- **Difference nearly-resonant sets:** Corresponding to the second Melnikov condition (1.7a), we define:

$$\Omega_{2,M}^{\tau,+} = \bigcup_{k \in \Lambda_{2M}} \bigcup_{\substack{j_1, j_2 = m+1 \\ j_1 \neq j_2}}^n \left\{ \omega_T \in \Omega \mid |\langle k, \omega_T \rangle - \omega_{j_1} + \omega_{j_2}| < \frac{1}{(|k|+2)^\tau} \right\}. \quad (3.7)$$

In this scheme, we do not need to consider the second case of the second Melnikov condition (1.7b) typically found in the classical KAM theorem.

For the total nearly-resonant set,  $\Omega_M^\tau = \Omega_{0,M}^\tau \cup \Omega_{1,M}^\tau \cup \Omega_{2,M}^{\tau,+}$ , we establish the following measure estimate, showing that the set of “bad” frequencies only occupies a negligible portion of the domain.

**Lemma 3.2.** Let  $\tau > m - 1$  be fixed. There exists a constant  $\kappa = \kappa(n, m, \tau, \Omega) > 0$ , depending on the dimension  $n$ , the tangent frequency dimension  $m$ , the parameter  $\tau$ , and the domain  $\Omega$ , such that the nearly-resonant set satisfies

$$\text{mes}(\Omega_M^\tau) \leq \kappa. \quad (3.8)$$

The proof is based on elementary measure estimates and is deferred to Section B.1.

### 3.2 Restricted operators on small boxes

In the small-scale regime, for tangent frequencies within the non-resonant set  $\Omega \setminus \Omega_M^\tau$ , we establish the invertibility and decay properties of the operator  $L$  restricted to central boxes. The following theorem verifies the implementation conditions for the restricted operator.

**Theorem 3.3.** Suppose  $\hat{z} \in \mathcal{K}(s)$  and  $\omega_T \in \Omega \setminus \Omega_M^\tau$ . Then the restricted operator  $L_N$  is invertible and satisfies the operator norm bound

$$\|L_N^{-1}\|_2 \leq \frac{1}{\varepsilon_N}. \quad (3.9)$$

Moreover, for any  $k \neq k'$ , its matrix entries satisfy the Gevrey decay estimate:

$$|L_N^{-1}(k, k')| \leq \exp\{-|k - k'|^s\} \leq \exp\left\{-\frac{|k - k'|^s}{2}\right\}. \quad (3.10)$$

By Theorem 2.5, the diagonal entries of  $D_N$  admit the uniform lower bound as

$$\begin{aligned} |D_{N;j,k}| &\geq |-\langle k, \omega_T \rangle + \omega_j| - |\langle k, \omega'_T - \omega_T \rangle| \\ &\geq \frac{1}{m^\tau N^\tau} - N \exp\{-(\log M)^{20}\} \geq \frac{1}{2m^\tau N^\tau}, \end{aligned} \quad (3.11)$$

for any  $k \in \Lambda_N \setminus \{e_j\}$  when  $j = 1, \dots, m$ , and any  $k \in \Lambda_N$  when  $j = m + 1, \dots, n$ , which ensures that  $D_N$  remains uniformly bounded away from zero. Consequently,  $(T + \varepsilon B)_N^{-1}$  can be estimated via a Neumann series. Since the off-diagonal terms involve only convolution operations preserving Gevrey decay, the proof follows from standard arguments and is deferred to Section B.2.

### 3.3 Verification of the implementation conditions

In this section, we demonstrate that the central restricted operator satisfies the implementation conditions (Theorem 3.1) within the large-scale regime  $N > M$ . We employ an inductive approach, utilizing Theorem 3.3 as the inductive base for the small-scale regime  $M_0 \leq N \leq M$ . Assume that for every scale  $N$  within the range  $M_0 \leq N \leq M^r$ , the central restricted operator satisfies the implementation conditions. Our objective is to prove that these conditions remain valid for the subsequent scales  $M^r < N \leq M^{r+1}$ . This inductive step relies on the analytical properties of the operator when restricted to the outer lattice boxes  $k_0 + \Lambda_N$ , where  $k_0 \notin \Lambda_{2N}$ . For brevity, we denote the restriction of the operator  $L$  to  $k_0 + \Lambda_N$  as  $L_{k_0, N}$ . The following theorem establishes its invertibility and off-diagonal decay properties to complete the induction. The proof, which leverages a multi-scale analysis framework, is detailed in Section 4.

**Theorem 3.4.** Suppose  $\hat{z} \in \mathcal{K}(s)$  and  $\omega_T \in \Omega \setminus (\Omega_M^r \cup G)$ , where  $G$  will be clarified in Section 4. Then for any  $k_0 \notin \Lambda_{2N}$ , the restricted operator  $L_{k_0, N}$  is invertible and satisfies:

$$\|L_{k_0, N}^{-1}\|_2 \leq \frac{1}{\varepsilon_N}. \quad (3.12)$$

Moreover, for any  $k, k' \in k_0 + \Lambda_N$  such that  $|k - k'| \geq N^{1/2}$ , the matrix entries satisfy:

$$\left| L_{k_0, N}^{-1}(k, k') \right| \leq \exp\left\{-\frac{|k - k'|^s}{2}\right\}. \quad (3.13)$$

To establish the implementation conditions at scale  $N$ , we set  $K = N^{1/10}$  and consider a central box  $\Lambda_{10K}$ . By the inductive hypothesis, the operator  $L$  restricted to the box  $\Lambda_{10K}$  satisfies the implementation conditions. We then introduce a subbox  $\Lambda_{9K} \subseteq \Lambda_{10K}$  and a family of translated boxes  $\{k + \Lambda_K\}$  where  $k \notin \Lambda_{9K}$ . Consequently, the lattice box  $\Lambda_N$  admits the following decomposition:

$$\Lambda_N = \Lambda_{10K} \cup \left( \bigcup_{k \notin \Lambda_{9K}} (k + \Lambda_K) \right), \quad (3.14)$$

where the properties established in Theorem 3.4 are applicable to the restricted operators  $L_{k, K}$ . We now demonstrate how to derive the global inverse  $L_N^{-1}$  using local information, specifically, the inverses of  $L$  restricted to  $\Lambda_{10K}$  and the family  $\{k + \Lambda_K\}$ .

**Central subbox** ( $k \in \Lambda_{9K}$ ) For lattice points within the central subbox, we partition the lattice as  $\Lambda_N = \Lambda_{10K} \cup \Lambda_{10K}^c$ , where  $\Lambda_{10K}^c = \Lambda_N \setminus \Lambda_{10K}$ . Applying the resolvent identity, we obtain the block representation:

$$\begin{pmatrix} L_{10K}^{-1} & 0 \\ 0 & L_{10K,-}^{-1} \end{pmatrix} = \left[ E + \varepsilon \begin{pmatrix} 0 & L_{10K}^{-1} P^* \\ L_{10K,-}^{-1} P & 0 \end{pmatrix} \right] \begin{pmatrix} (L_N^{-1})_{\Lambda_{10K} \times \Lambda_{10K}} & (L_N^{-1})_{\Lambda_{10K} \times \Lambda_{10K}^c} \\ (L_N^{-1})_{\Lambda_{10K}^c \times \Lambda_{10K}} & (L_N^{-1})_{\Lambda_{10K}^c \times \Lambda_{10K}^c} \end{pmatrix}, \quad (3.15)$$

where  $P$  and  $P^*$  are coupling operators generated from  $B + S$ , and  $L_{10K,-}^{-1}$  denotes the inverse of the operator  $L$  restricted to  $\Lambda_{10K}^c$ . From the relation, the components are expressed as:

$$\begin{cases} (L_N^{-1})_{\Lambda_{10K} \times \Lambda_{10K}} = L_{10K}^{-1} - \varepsilon L_{10K}^{-1} P^* (L_N^{-1})_{\Lambda_{10K}^c \times \Lambda_{10K}}, \\ (L_N^{-1})_{\Lambda_{10K} \times \Lambda_{10K}^c} = -\varepsilon L_{10K}^{-1} P^* (L_N^{-1})_{\Lambda_{10K}^c \times \Lambda_{10K}^c}. \end{cases} \quad (3.16a)$$

$$(L_N^{-1})_{\Lambda_{10K} \times \Lambda_{10K}^c} = -\varepsilon L_{10K}^{-1} P^* (L_N^{-1})_{\Lambda_{10K}^c \times \Lambda_{10K}^c}. \quad (3.16b)$$

By gluing (3.16a) and (3.16b) and extending the terms to the full index set  $\Lambda_N$ , we derive

$$(L_N^{-1})_{\Lambda_{10K} \times \Lambda_N} = \begin{pmatrix} L_{10K}^{-1} & 0 \\ 0 & (L_{10K}^{-1} P^*) \end{pmatrix} L_N^{-1}. \quad (3.17)$$

Utilizing the inductive assumption alongside Theorem 2.2 and Theorem 2.4, we establish upper bounds for the operator  $L_{10}^{-1} P^*$ . For any  $k \in \Lambda_{9K}$  and  $k' \notin \Lambda_{10K}$ , the distance satisfies  $|k - k'| \geq K$ . Consequently, the entries of  $(L_{10}^{-1} P^*)(k, k')$  exhibits Gevrey decay. Specifically, by decomposing the region into short-range and long-range domains, the entries satisfy:

$$|(L_{10K}^{-1} P^*)(k, k')| \leq \begin{cases} \exp \left\{ -\frac{|k - k'|^s}{2} \right\}, & \text{if } |k' - k| < 100K, \\ \exp \left\{ -\frac{3|k - k'|^s}{4} \right\}, & \text{if } |k' - k| \geq 100K. \end{cases} \quad (3.18)$$

Finally, by restricting the identity (3.17) to the subset  $\Lambda_{9K} \times \Lambda_N$ , we arrive at:

$$(L_N^{-1})_{\Lambda_{9K} \times \Lambda_N} = \begin{pmatrix} L_{10K}^{-1} & 0 \\ 0 & (L_{10K}^{-1} P^*) \end{pmatrix}_{\Lambda_{9K} \times \Lambda_N} L_N^{-1}, \quad (3.19)$$

where the entries of  $(L_{10K}^{-1} P^*)_{\Lambda_{9K} \times \Lambda_{10K}^c}$  satisfy the Gevrey decay conditions (3.18).

**Outer boxes** ( $k \notin \Lambda_{9K}$ ) For lattice points outside the central subbox, we partition the lattice as  $\Lambda_N = (k + \Lambda_K) \cup (k + \Lambda_K)^c$ , where  $(k + \Lambda_K)^c = \Lambda_N \setminus (k + \Lambda_K)$ . Following a block representation and resolvent identity procedure analogous to (3.16) — (3.19), we establish

$$(L_N^{-1})_{\{k\} \times \Lambda_N} = \begin{pmatrix} (L_{k,K}^{-1})_{\{k\} \times (k + \Lambda_K)} & 0 \\ 0 & (L_{k,K}^{-1} P^*)_{\{k\} \times (k + \Lambda_K)^c} \end{pmatrix} L_N^{-1}, \quad (3.20)$$

where the entries of  $(L_{k,K}^{-1} P^*)_{\{k\} \times (k + \Lambda_K)^c}$  satisfy the Gevrey decay estimate:

$$|(L_{10K}^{-1} P^*)(k, k')| \leq \begin{cases} \exp \left\{ -\frac{|k - k'|^s}{2} \right\}, & \text{if } |k' - k| < 4K, \\ \exp \left\{ -\frac{3|k - k'|^s}{4} \right\}, & \text{if } |k' - k| \geq 4K. \end{cases} \quad (3.21)$$

By combining (3.19) and (3.20), the global inverse can be expressed as

$$L_N^{-1} = \Psi_N - \varepsilon \Phi_N L_N^{-1}, \quad (3.22)$$

where the operator  $\Psi_N$  is constructed from the lower-scale inverses,  $L_{10K}^{-1}$  and  $L_{k,K}^{-1}$ , as follows:

$$\Psi_N(k, k') = \begin{cases} L_{10K}^{-1}(k, k'), & \text{if } k \in \Lambda_{9K}, k' \in \Lambda_{10K}, \\ L_{k,K}^{-1}(k, k'), & \text{if } k \notin \Lambda_{9K}, k' - k \in \Lambda_K, \\ 0, & \text{otherwise.} \end{cases} \quad (3.23)$$

Based on the estimates provided in (3.18) and (3.21), the entries of the operator  $\Phi_N$  satisfy:

$$\Phi_N(k, k') \leq \begin{cases} 0, & \text{if } k = k'; \\ \exp\left\{-\frac{|k - k'|^s}{2}\right\}, & \text{if } 0 < |k' - k| < 100K; \\ \exp\left\{-\frac{3|k - k'|^s}{4}\right\}, & \text{if } |k' - k| \geq 100K. \end{cases} \quad (3.24)$$

For a sufficiently small  $\varepsilon$ , the operator  $E + \varepsilon\Phi_N$  is invertible via the Neumann series expansion. For long-range interactions where  $|k - k'| \geq N^{1/4}$ , the inverse satisfies:

$$|(E + \varepsilon\Phi_N)^{-1}(k, k')| \leq \exp\left\{-\frac{|k - k'|^s}{2} - \frac{1}{4}(100K)^s\right\}, \quad (3.25)$$

where this bound accounts for interaction paths containing at least one long-range jump. If a path consisted solely of short-range interactions to cover the distance  $|k - k'|$ , the ‘‘cost’’ (the cumulative decay exponent) would be even higher. Specifically, according to the concavity property for  $s < 1$ , the total index must satisfy:

$$\frac{|k - k'|}{100K}(100K)^s \geq \left(\frac{N^{1/4}}{100K}\right)^{1-s} \cdot |k - k'|^s \geq |k - k'|^s + \frac{1}{2}(100K)^s$$

A more refined analysis for the Gevrey case reveals that the inverse  $(E + \varepsilon\Phi_N)^{-1}(k, k')$  preserves short-range decay, while the long-range decay follows (3.24) with the transition threshold shifted from  $100K$  to  $K^2$ . In contrast, the concavity property is unavailable in the analytic case. Consequently, the parameter  $\varepsilon$  must be more strictly tuned to compensate for the lack of sub-linear exponent growth and to ensure sufficient decay for purely short-range interaction paths. We can thus rewrite (3.22) as

$$L_N^{-1} = (E + \varepsilon\Phi_N)^{-1}\Psi_N. \quad (3.26)$$

Finally, by (3.23), the  $\ell_2$ -norm satisfies  $\|\Psi_N\|_2 \leq (20K)^m \exp\{(\log(10K))^{15}\}$ . By substituting this bound together with (3.25) into (3.26), we conclude that  $L_N^{-1}$  satisfies the implementation conditions at scale  $N$ .

## 4 Multi-scale analysis

In this section, we employ a multi-scale analysis to establish Theorem 3.4 for the ‘‘outer’’ boxes  $k_0 + \Lambda_N$ , where the center satisfies  $k_0 \notin \Lambda_{2N}$ . For any indices  $k, k' \in k_0 + \Lambda_N$ , the condition  $k_0 \notin \Lambda_{2N}$  implies a lower bound of  $|k| + |k'| \geq 2N$ . Consequently, the restricted operator satisfies the following norm estimate:

$$\|B_{k_0, N}\|_2 \leq \sqrt{\|B_{k_0, N}\|_1 \cdot \|B_{k_0, N}\|_\infty} \leq (2N + 1)^m \exp\{-N^s\}.$$

Given that  $T_{k_0,N} = D_{k_0,N} + \varepsilon S_{k_0,N}$  is symmetric with respect to the indices  $k$  and  $k'$ , we analyze the numerical operator  $L_{k_0,N} = T_{k_0,N} + \varepsilon B_{k_0,N}$ . When the smallest eigenvalue of  $T_{k_0,N}$  scales as  $\exp(-(\log N)^s)$  for  $s > 0$ , we examine the product

$$L_{k_0,N}^\top L_{k_0,N} = T_{k_0,N}^2 + \varepsilon(B_{k_0,N}^\top T_{k_0,N} + T_{k_0,N} B_{k_0,N}) + \varepsilon^2 B_{k_0,N}^\top B_{k_0,N}.$$

Due to the rapid decay of  $B_{k_0,N}$  established above, the perturbation terms are negligible compared to the leading term  $T_{k_0,N}^2$ . Therefore, obtaining a robust bound for  $\|T_{k_0,N}^{-1}\|_2$  is sufficient to control the inverse norm  $\|L_{k_0,N}^{-1}\|_2$ .

For the remainder of this section, we focus on estimating  $T_{k_0,N}^{-1}$ . Since the specific location of the center  $k_0 \notin \Lambda_{2N}$  does not explicitly affect the subsequent analysis, we omit the subscript  $k_0$  unless otherwise specified and simplify the notation by setting  $\Gamma_N = k_0 + \Lambda_N$ ,  $T_N := T_{k_0,N}$ , and  $D_N := D_{k_0,N}$ .

#### 4.1 Inductive base for small boxes

We begin the multi-scale analysis by considering the small-scale regime  $M_0 \leq N \leq M$ . According to Theorem 2.5, the gap between any two eigenvalues of  $D_N$  satisfies the following lower bound:

$$|D_{N;j_1,k_1} - D_{N;j_2,k_2}| = |-\langle k_1 - k_2, \omega'_T \rangle + \omega_{j_1} - \omega_{j_2}| \geq |-\langle k_1 - k_2, \omega_T \rangle + \omega_{j_1} - \omega_{j_2}| - 2N\varepsilon. \quad (4.1)$$

For any tangent frequency  $\omega_T \in \Omega \setminus \Omega_M^\tau$ , we exploit the fact that  $\varepsilon$  is “super-polynomially” small, specifically, it decays faster than any polynomial in  $N$ . This leads to several key observations regarding the resonance conditions. First, when the normal frequency difference is not zero, the definitions of the single-mode resonant sets (3.6) and the difference resonant sets (3.7) imply that the gap condition can only fail if  $j_1 = j_2$  and  $k_1 = k_2$ . Hence, for distinct eigenvalues, the normal frequency components must vanish. Furthermore, the tangent resonant set defined in (3.5) ensures that the gap condition is violated by  $(k_1 - e_{j_1}) - (k_2 - e_{j_2}) = 0$ . Given that  $j = 1, \dots, m$ , there exists at most  $m$  entries of  $D_n$  falling below the threshold  $(4mN)^{-\tau}$ , which is formalized in the following proposition.

**Proposition 4.1.** Suppose that  $\hat{z} \in \mathcal{K}(s)$  and the tangent frequency satisfies  $\omega_T \in \Omega \setminus \Omega_M^\tau$ . Then the diagonal operator  $D_N$  admits at most  $m$  entries  $D_{N;j,k} = -\langle k, \omega'_T \rangle + \omega_j$  for  $j = 1, \dots, n$ , whose absolute value is smaller than  $(4mN)^{-\tau}$ .

For entries falling below the threshold  $(4mN)^{-\tau}$ , the indices  $k_j - e_j$  for  $j = 1, \dots, m$  remain fixed. For convenience, we denote this fixed index as  $k_\star = k_j - e_j$ . We then define the set of these entries as

$$\Xi = \{-\langle k_\star, \omega'_T \rangle + \omega_j - \omega'_j \mid j = 1, \dots, m\}. \quad (4.2)$$

This index set identifies the singular site, a singleton set denoted as  $\Pi = \{k_\star\}$ . To establish the inductive base in the small-scale regime, we formulate the following two lemmas. First, we consider the operator  $T$  restricted to the index set excluding the singular site,  $\Gamma_N \setminus \Pi$ . By applying Theorem 4.1 and following a procedure similar to the proof of Theorem 3.3, we derive the following bounds for its inverse.

**Lemma 4.2.** Suppose that  $\hat{z} \in \mathcal{K}(s)$  and  $\omega_T \in \Omega \setminus \Omega_M^\tau$ . The restricted operator  $T_{\Gamma_N \setminus \Pi}$  is invertible, and its inverse satisfies the operator norm bound

$$\|T_{\Gamma_N \setminus \Pi}^{-1}\|_2 \leq \frac{1}{\varepsilon_N}. \quad (4.3)$$

In addition, the off-diagonal entries of  $T_{\Gamma_N \setminus \Pi}^{-1}$  satisfy the decay estimate

$$\left| T_{\Gamma_N \setminus \Pi}^{-1}(k, k') \right| \leq \exp \left\{ -\frac{|k - k'|^s}{2} \right\}, \quad (4.4)$$

for any  $k \neq k' \in \Gamma_N \setminus \Pi$ .

Next, we analyze  $T_N^{-1}$  by leveraging the properties of  $T_{\Gamma_N \setminus \Pi}^{-1}$ . According to the resolvent identity, we express the block structure of the inverse as follows:

$$\begin{pmatrix} T_{\Gamma_N \setminus \Pi}^{-1} & 0 \\ 0 & T_{\Pi}^{-1} \end{pmatrix} = \left[ E + \varepsilon \begin{pmatrix} 0 & T_{\Gamma_N \setminus \Pi}^{-1} P^* \\ T_{\Pi}^{-1} P & 0 \end{pmatrix} \right] \begin{pmatrix} (T_N^{-1})_{(\Gamma_N \setminus \Pi) \times (\Gamma_N \setminus \Pi)} & (T_N^{-1})_{(\Gamma_N \setminus \Pi) \times \Pi} \\ (T_N^{-1})_{\Pi \times (\Gamma_N \setminus \Pi)} & (T_N^{-1})_{\Pi \times \Pi} \end{pmatrix}. \quad (4.5)$$

Since  $T_N$  is symmetric with respect to the indices  $k$  and  $k'$ , the identity (4.5) yields the relation:

$$(T_N^{-1})_{\Pi \times (\Gamma_N \setminus \Pi)}^\top = (T_N^{-1})_{(\Gamma_N \setminus \Pi) \times \Pi} = -\varepsilon T_{\Gamma_N \setminus \Pi}^{-1} P^* (T_N^{-1})_{\Pi \times \Pi}. \quad (4.6)$$

If the inverse is bounded, specifically,  $\|T_N^{-1}\|_2 \leq \varepsilon_N^{-1}$ , the relation (4.6) implies the localization condition. We thus establish that, within the small-scale regime, the existence of an inverse with exponential-logarithmic growth implies localization.

**Lemma 4.3.** Suppose that  $\hat{z} \in \mathcal{K}(s)$  and  $\omega_T \in \Omega \setminus \Omega_M^T$ . If the restricted operator  $T_N$  is invertible and satisfies the operator norm bound

$$\|T_N^{-1}\|_2 \leq \frac{1}{\varepsilon_N}, \quad (4.7)$$

then the off-diagonal entries of  $T_N^{-1}$  satisfy the decay estimate

$$\left| T_N^{-1}(k, k') \right| \leq \exp \left\{ -\frac{|k - k'|^s}{2} \right\}, \quad (4.8)$$

for any  $k \neq k' \in \Gamma_N$ .

In the small-scale regime, the growth of  $\varepsilon_N^{-1}$  is suppressed by the small parameter  $\varepsilon$ . In the large-scale regime, however, this mechanism is no longer sufficient; the growth of  $\varepsilon_N^{-1}$  is instead counteracted by the Gevrey decay of the interaction terms originating from  $P^*$ .

## 4.2 Size reduction: clustering of singular sites

In this section, we analyze the eigenvalues of the restricted operator  $T_N$ , which are given by

$$T_{N;j,k} = -\langle k, \omega'_T \rangle + \omega_j + \mu_{j,k}(\omega'_T). \quad (4.9)$$

Based on the results established in Theorem 2.2, the perturbation term  $\mu_{j,k}$  is bounded. Specifically, it satisfies the following gradient estimate:

$$\max_{j=1, \dots, n} \max_{k \in \mathbb{Z}^m} \left\| \frac{\partial \mu_{j,k}}{\partial \omega'_T} \right\|_2 \leq \varepsilon \left\| \frac{\partial S}{\partial \omega'_T} \right\|_2 \leq \frac{\varepsilon}{2}. \quad (4.10)$$

Recall from Theorem 2.5 that the mapping between the tangent frequencies  $\omega_T$  and  $\omega'_T$  is a diffeomorphism. Given that the normal frequencies  $\omega_j$  (for  $j = m + 1, \dots, n$ ) are differentiable with respect to  $\omega'_T$ , we conclude there exists a constant  $K > 0$  such that:

$$\max_{j=1, \dots, n} \left\| \frac{\partial \omega_j}{\partial \omega'_T} \right\|_2 \leq K. \quad (4.11)$$

We now examine the difference between any two eigenvalues of  $T_N$ :

$$T_{N;j_1, k_1} - T_{N;j_2, k_2} = -\langle k, \omega'_T \rangle + \omega_{j_1} - \omega_{j_2} + \mu_{j_1, k_1}(\omega'_T) - \mu_{j_2, k_2}(\omega'_T) \quad (4.12)$$

where  $k = k_1 - k_2$ . To resolve the small divisor problem, we exclude the resonant regions along the direction  $k/\|k\|_2$ . Using the bounds established in (4.10) and (4.11), we observe that when  $\|k\|_2$  is sufficiently large, the same excision procedure as in the unperturbed case applies. When the perturbation vanishes and the drifted tangent frequency  $\omega'_T$  degenerates to  $\omega_T$ , the curved resonance regions “straighten out” into the nearly-resonant sets defined in (3.5), (3.6), and (3.7), which is shown in Figure 1.

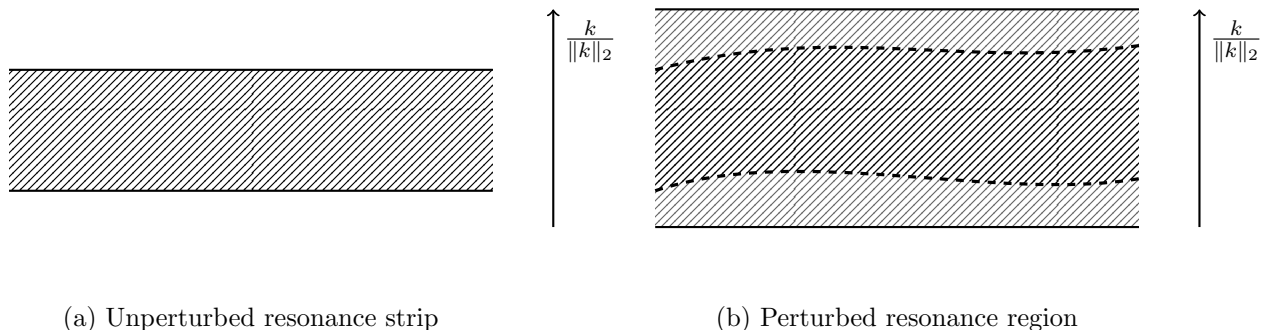


Figure 1: Geometric illustration of resonance regions. In (b), the solid lines denote the boundaries of the excluded strip, while the dashed curves delineate the perturbed resonant region arising from the variation of the term  $\mu_{j,k}$ .

Following the intuitive description above, we now introduce the rigorous scaling parameters and nearly-resonance sets required for the large-scale regime where  $N > M$ . We begin by defining a reduced scale  $N'$ , derived from the primary scale  $N$  via the following polylogarithmic relation:

$$N' = \exp \left\{ (\log N)^{\frac{1}{10}} \right\}. \quad (4.13)$$

We next define the difference nearly-resonant set for the large-scale regime as the union of its components across all scales  $N > M$ .

**Definition 4.4.** The difference nearly-resonant set in the large-scale regime is given by

$$G_2 = \bigcup_{N > M} G_{2,N}$$

where each component set  $G_{2,N}$  is defined as:

$$G_{2,N} = \bigcup_{j_1, j_2=1}^n \bigcup_{k \in \Lambda_{2N} \setminus \Lambda_{2N'}} \left\{ \omega_T \in \Omega \left| |-\langle k, \omega'_T \rangle + \omega_{j_1} - \omega_{j_2} + \mu_{j_1, k_1} - \mu_{j_2, k_2}| < 2\varepsilon_{N'} \right. \right\}. \quad (4.14)$$

Based on the scaling relation in (4.13), the total measure satisfies

$$\text{mes}(G_2) = \sum_{N > M} (2N + 1)^m \exp \left\{ -(\log N)^{\frac{3}{2}} \right\} < \infty.$$

In particular, as  $\varepsilon \rightarrow 0$ , it follows that  $M \rightarrow \infty$ , which implies  $\text{mes}(G_2) \rightarrow 0$ .

Consider the operator  $T$  restricted to two boxes,  $k_{0,1} + \Lambda_{N'}$  and  $k_{0,2} + \Lambda_{N'}$ , centered at  $k_{0,1}, k_{0,2} \in \Gamma_N$ . If the two centers satisfy the separation condition  $|k_{0,1} - k_{0,2}| \geq 4N'$ , then at least one of the restricted operators  $T_{k_{0,1}, N'}$  and  $T_{k_{0,2}, N'}$  has its smallest eigenvalue (in absolute value) bounded below by  $\varepsilon_{N'}$ . Equivalently, at most one of the resolvent norms,  $\|T_{k_{0,1}, N'}^{-1}\|_2$  or  $\|T_{k_{0,2}, N'}^{-1}\|_2$ , can exceed  $\varepsilon_{N'}^{-1}$ . To formalize this spatial clustering, we define the set of ‘‘singular’’ centers within the domain  $\Gamma_N$  as

$$\Sigma(N, N') = \left\{ k \in \Gamma_N \left| \|T_{k, N'}^{-1}\|_2 > \frac{1}{\varepsilon_{N'}} \right. \right\}. \quad (4.15)$$

The spatial distribution of these singular centers is characterized by the following lemma.

**Lemma 4.5.** Suppose that  $\hat{z} \in \mathcal{K}(s)$  and  $\omega_T \in \Omega \setminus (\Omega_M^T \cup G_2)$ . If two box centers satisfy  $k_{0,1}, k_{0,2} \in \Sigma(N, N')$ , then they must be clustered such that:

$$k_{0,1} - k_{0,2} \in \Lambda_{4N'}.$$

### 4.3 Multi-scale induction: inversion implies localization

Based on Theorem 4.5, we establish the inclusion  $\Sigma(N, N') \subseteq \Gamma_{4N'}$ , which is subsequently contained within  $\Gamma_{10N'}$ . For the purpose of our decomposition, we designate  $\Gamma_{10N'}$  as the singular box. Accordingly, any box whose center lies outside  $\Sigma(N, N')$  is referred to as a regular box. With this classification, we decompose the box  $\Gamma_N$  into a singular box together with a collection of regular boxes:

$$\Gamma_N = \Gamma_{10N'} \cup \left( \bigcup_{k \notin \Gamma_{9N'}} (k + \Lambda_{N'}) \right). \quad (4.16)$$

where the choice of size  $10N'$  rather than  $4N'$  is deliberate. Indeed, any box  $k + \Lambda_{N'}$  centered at  $k \in \Gamma_{10N'} \setminus \Gamma_{9N'}$  is still treated as regular. This enlargement facilitates the subsequent gluing procedure, consistent with the strategy detailed in Section 3.3.

We repeat the scale reduction process for each box in the decomposition (4.16). This iteration continues through a sequence of scales satisfying the hierarchy in (4.13) until they reach the small-scale regime  $[M_0, M]$ . For the singular box, Theorem 4.1 ensures that the set of singular sites is a singleton,  $\Pi = \{k_\star\}$ . Within this small-scale regime, we have established the following results.

- (i) For the singular box excluding the singular site  $\Pi$ , Theorem 4.2 guarantees that the inversion condition (4.3) and the localization conditions (4.4) hold simultaneously.

- (ii) For the regular boxes, Theorem 4.3, we establishes that the inversion condition (4.7) directly implies the localization condition (4.8).

With these small-scale results serving as the inductive bases, we establish that inversion implies localization across the large-scale regime  $N > M$ , rigorously stated as the following lemma.

**Lemma 4.6.** Suppose that  $\hat{z} \in \mathcal{K}(s)$  and  $\omega_T \in \Omega \setminus (\Omega_M^r \cup G_2)$ . If the restricted operator  $T_N$  satisfies the inversion condition (4.7) for any  $M^r < N \leq M^{r+1}$ , then the entries of its inverse satisfies the localization condition

$$|T_N^{-1}(k_1, k_2)| \leq \exp \left\{ -\frac{|k_1 - k_2|^s}{2} \right\} \quad (4.17)$$

for any  $|k_1 - k_2| \geq N^{\frac{1}{2}}$ .

The proof consists of two successive steps: first, a “gluing” process following the procedure as detailed in Section 3.3; and second, a demonstration that inversion implies localization, which remains entirely consistent with (4.5) and (4.6).

**The “gluing” procedure** We begin by considering the set  $\Gamma_N \setminus \Pi$  at a scale satisfying  $M^r \leq N \leq M^{r+1}$ . According to (4.16), the set  $\Gamma_N \setminus \Pi$  can be decomposed as:

$$\Gamma_N \setminus \Pi = (\Gamma_{10N'} \setminus \Pi) \cup \left( \bigcup_{k \notin \Gamma_{9N'}} (k + \Lambda_{N'}) \right). \quad (4.18)$$

By the inductive hypothesis for  $M_0 \leq N \leq M^r$ , the following holds:

- The operator restricted to the central region  $\Gamma_{10N'} \setminus \Pi$ , with a scale satisfying  $M_0 \leq 4N' \leq M^r$ , fulfills the inversion condition (4.3) and the localization condition (4.4).
- The operator restricted to each outer box  $k + \Lambda_{N'}$ , where  $M_0 \leq N' \leq M^r$ , satisfies the property that the inversion condition (4.7) directly implies the localization condition (4.8).

By applying the same resolvent identity framework developed in (3.15) — (3.19), we can derive the following representation for the inverse operator restricted to  $\Gamma_{9N'} \setminus \Pi \times \Gamma_N$  as

$$\left( T_{\Gamma_{10N'} \setminus \Pi}^{-1} \right)_{(\Gamma_{9N'} \setminus \Pi) \times \Gamma_N} = \left( T_{\Gamma_{10N'} \setminus \Pi}^{-1} \quad 0 \right)_{(\Gamma_{9N'} \setminus \Pi) \times \Gamma_N} - \varepsilon \left( 0 \quad \left( T_{\Gamma_{10N'} \setminus \Pi}^{-1} P^* \right) \right)_{(\Gamma_{9N'} \setminus \Pi) \times \Gamma_N} T_N^{-1}, \quad (4.19)$$

where the entries of  $(T_{\Gamma_{10N'} \setminus \Pi}^{-1} P^*)_{(\Gamma_{9N'} \setminus \Pi) \times (\Gamma_{10N'} \setminus \Pi)^c}$  exhibit the Gevrey decay. Specifically, these entries satisfy the following decay estimates across the short-range and long-range domains:

$$|(T_{\Gamma_{10N'} \setminus \Pi}^{-1} P^*)(k, k')| \leq \begin{cases} \exp \left\{ -\frac{|k - k'|^s}{2} \right\}, & \text{if } |k' - k| < 100N', \\ \exp \left\{ -\frac{3|k - k'|^s}{4} \right\}, & \text{if } |k' - k| \geq 100N'. \end{cases} \quad (4.20)$$

Similarly, for a singleton  $\{k\}$  within the outer boxes, the inverse is represented as:

$$(T_{k, N'}^{-1})_{\{k\} \times \Gamma_N} = \left( (T_{k, N'}^{-1})_{\{k\} \times (k + \Lambda_{N'})} \quad 0 \right) - \varepsilon \left( 0 \quad (T_{k, N'}^{-1} P^*)_{\{k\} \times (k + \Lambda_{N'})^c} \right) T_N^{-1}, \quad (4.21)$$

where the corresponding Gevrey decay for these entries is:

$$|(T_{\Gamma_{10N'} \setminus \Pi}^{-1} P^*)(k, k')| \leq \begin{cases} \exp \left\{ -\frac{|k - k'|^s}{2} \right\}, & \text{if } |k' - k| < 4N', \\ \exp \left\{ -\frac{3|k - k'|^s}{4} \right\}, & \text{if } |k' - k| \geq 4N'. \end{cases} \quad (4.22)$$

Following the same procedure established in (3.22) – (3.26), we derive the unified representation:

$$T_{\Gamma_N \setminus \Pi}^{-1} = (E - \varepsilon \Phi_N)^{-1} \Psi_N, \quad (4.23)$$

which confirms that  $\|T_{\Gamma_N \setminus \Pi}^{-1}\|_2 \leq \exp \{(\log 10N')^{15}\} < \exp \{(\log N)^{15}\}$  and that the entries satisfy the Gevrey decay condition (4.4). Furthermore,  $T_{\Gamma_N \setminus \Pi}$  satisfies Theorem 4.2 at the scale  $M^r < N \leq M^{r+1}$ .

**Inversion implies localization** We now establish Theorem 4.3 for the scale  $M^r < N \leq M^{r+1}$ . At this scale, the relation (4.6) is maintained as follows:

$$(T_N^{-1})_{\Pi \times (\Gamma_N \setminus \Pi)}^\top = (T_N^{-1})_{(\Gamma_N \setminus \Pi) \times \Pi} = -\varepsilon T_{\Gamma_N \setminus \Pi}^{-1} P^* (T_N^{-1})_{\Pi \times \Pi}$$

Building upon Theorem 4.2 and assuming that the inversion condition (4.7) holds, we derive the localization condition (4.8). It is important to note that the parameter  $\varepsilon$  is insufficient to suppress the growth of  $(T_N^{-1})_{\Pi \times \Pi}$  at large scales. Instead, the proof relies crucially on the Gevrey decay inherited from the off-diagonal operator  $P^*$ , which effectively counteracts the exponential polylogarithmic growth, ensuring that localization properties are preserved across the entire domain.

#### 4.4 Measure estimate for “bad” frequencies

The final stage of our analysis involves quantifying the set of “bad” frequencies, those that must be excluded to ensure the inversion condition (4.7) remains valid. In this section, we establish the rigorous measure estimates for these resonant sets. Recall that the restricted operator  $T_N$  admits the following block decomposition:

$$T_N = \begin{pmatrix} T_{\Gamma_N \setminus \Pi} & \varepsilon P^* \\ \varepsilon P & T_\Pi \end{pmatrix}.$$

By analyzing this block structure, we identify the Schur complement with respect to  $T_\Pi$  as:

$$U = T_\Pi - \varepsilon^2 P T_{\Gamma_N \setminus \Pi}^{-1} P^*. \quad (4.24)$$

Based on the Schur complement defined in (4.24), we establish an upper bound for the  $\ell_2$ -norm of the inverse operator:

$$\|T_N^{-1}\|_2 \leq 4 \|T_{\Gamma_N \setminus \Pi}^{-1}\|_2^2 \cdot \|U^{-1}\|_2 + \|T_{\Gamma_N \setminus \Pi}^{-1}\|_2.$$

Given the established bound  $\|T_{\Gamma_N \setminus \Pi}^{-1}\|_2 \leq \exp \{(\log 10N')^{15}\}$ , we derive the following inclusion for the resonant sets:

$$\left\{ \omega_T \in \Omega \left| \|T_N^{-1}\|_2 > \frac{1}{\varepsilon_N} \right. \right\} \subseteq \left\{ \omega_T \in \Omega \left| \|U^{-1}\|_2 > \frac{1}{\sqrt{\varepsilon_N}} \right. \right\}, \quad (4.25)$$

which implies that analyzing the Schur complement  $U$  is sufficient for our measure estimates. Thus, we further expand the Schur complement (4.24) as

$$U = \text{diag}(-\langle k_\star, \omega'_T \rangle + \omega_j) + \varepsilon S(k_\star, k_\star) - \varepsilon^2 P T_{\Gamma_N \setminus \Pi}^{-1} P^*.$$

By introducing the shift parameter  $\sigma_\star = -\langle k_\star, \omega'_T \rangle$ , we define the residual term as:

$$\Upsilon = \text{diag}(\omega_j) + \varepsilon S(k_\star, k_\star) - \varepsilon^2 P T_{\Gamma_N \setminus \Pi}^{-1} P^*$$

Given that  $\|T_{\Gamma_N \setminus \Pi}^{-1}\|_2 \leq \exp\{(\log 10N')^{15}\}$ , it follows that  $\|\Upsilon\|_2 \leq \exp\{(\log 10N')^{15}\}$ . Consequently, we can express the Schur complement from (4.24) in the simplified form:

$$U = \sigma_\star E + \Upsilon, \quad (4.26)$$

where, to verify the implementation conditions detailed in Section 3.3, there is one and only one singular site within each outer box of the decomposition (3.14). Combining (4.25) and (4.26), we define the single-mode nearly-resonant set at the scale  $N$  as:

$$G_{1,N} = \bigcup_{k \in \Lambda_{N10}} \left\{ \omega_T \in \Omega \mid |\sigma_\star| - \|\Upsilon\|_2 < \sqrt{\varepsilon_N} \right\}, \quad (4.27)$$

which ensures that the inversion condition (4.7) holds for all tangent frequencies  $\omega_T \notin G_{1,N}$ . To estimate the measure of this set, we utilize a simplified version of the Cartan estimate [Levin, 1996].

**Lemma 4.7** (Theorem 4 of Lecture 11.3 in Levin [1996]). Let  $f(x)$  be a function analytic in the disk  $\{z : |z| \leq 2eR\}$ ,  $|f(0)| = 1$ , and let  $\eta$  be an arbitrary small positive number. We use the notation  $M_f(r) := \max_{|z|=r} |f(z)|$ . Then the estimate

$$\log |f(z)| > -H(\eta) \log M_f(2eR), \quad H(\eta) = \log \frac{15e^3}{\eta},$$

is valid everywhere in the disk  $\{z : |z| \leq R\}$  except a set of disks  $(C_j)$  with sum of radii

$$\sum r_j \leq \eta R.$$

To complete the measure estimates, we analyze the magnitude of the residual term  $\Upsilon$  across two distinct regimes. For small residuals, given by  $\|\Upsilon\|_2 < \sqrt{\varepsilon_N}$ , the single-mode nearly-resonant set is contained within

$$G_{1,N} \subseteq \bigcup_{k \in \Lambda_{N10}} \left\{ \omega_T \in \Omega \mid |\sigma_\star| < 2\sqrt{\varepsilon_N} \right\}. \quad (4.28)$$

Note that this case encompasses the small-scale regimes, where the tighter condition  $|\sigma_\star| < \varepsilon_N$  is actually sufficient. The measure for this regime is bounded by:

$$\text{mes}(G_{1,N}) \leq 2^{m+2} d^{m-1} (2N^{10} + 1)^m \sqrt{\varepsilon_N}. \quad (4.29)$$

When the residual term is large, i.e.,  $\|\Upsilon\|_2 \geq \sqrt{\varepsilon_N}$ , we define an analytic function:

$$f(\sigma_\star) = \frac{|\sigma_\star|}{\|\Upsilon\|_2} - 1.$$

with the disk parameter set as  $\|\Upsilon\|_2 = 2e(1+e)^{-1}R$ . It follows that  $|f(0)| = 1$  and  $M_f(2eR) = e$ . Accordingly, the single-mode nearly-resonant set satisfies:

$$G_{1,N} \subseteq \bigcup_{k \in \Lambda_{N^{10}}} \left\{ \omega_T \in \Omega \mid |f(\sigma_*)| < \varepsilon_N^{1/4} \right\}. \quad (4.30)$$

By setting  $\eta = 15e^3\varepsilon_N^{1/4}$ , Theorem 4.7 provides the following measure estimate:

$$\text{mes}(G_{1,N}) \leq 8(1+e)e^2(2N^{10}+1)^m \varepsilon_N^{1/4}. \quad (4.31)$$

Based on (4.27), the total single-mode resonant set is the union across all scales  $N \geq M_0$  as

$$G_1 = \bigcup_{N \geq M_0} G_{1,N}. \quad (4.32)$$

Synthesizing the estimates from (4.29) and (4.31), we derive

$$\text{mes}(G_1) \leq \sum_{N \geq M_0} 2^{m+2} d^{m-1} (2N^{10}+1)^m \varepsilon_N^{1/4} < \infty.$$

Notably, as  $\varepsilon \rightarrow 0$ , it follows  $M_0 \rightarrow \infty$ , which implies  $\text{mes}(G_1) \rightarrow 0$ . The combined set  $G = G_1 \cup G_2$  corresponds to the set defined in Theorem 3.4. Consequently, we obtain  $\text{mes}(G) \leq \delta$ , where  $\delta \rightarrow 0$  as  $\varepsilon \rightarrow 0$ , consistent with the statement of Theorem 1.1.

## 5 Convergence of the numerical scheme

In this section, we establish the theoretical foundation for the convergence of the proposed numerical scheme (1.18). Section 5.1 derives the iteration lemma, which serves as the technical cornerstone of our analysis. Subsequently, in Section 5.2, we utilize this result to complete the formal proof of the main statement.

### 5.1 The iteration lemma

Before proceeding to the inductive estimates, we must characterize the derivative of the inverse operator  $\partial L_N^{-1}$ , specifically regarding its norm bounds and off-diagonal decay properties. Here, the derivative is taken with respect to the tangent frequency  $\omega_T$ , which we omit from the notation for simplicity. Using the standard operator identity  $L_N^{-1} L_N = I$ , the derivative of the inverse is given by:

$$\partial L_N^{-1} = -L_N^{-1} (\partial L_N) L_N^{-1}. \quad (5.1)$$

This relationship allows us to establish the following lemma regarding the operator's composite norm and spatial localization.

**Lemma 5.1.** If the restricted operator  $L_N$  satisfies Theorem 3.1, then its inverse satisfies the norm bound:

$$\|\partial L_N^{-1}\|_2 \leq \frac{4\sqrt{m}N}{\varepsilon_N^2}. \quad (5.2)$$

Furthermore, for sufficiently large spatial separations in the lattice  $\Lambda_N$ , specifically when  $|k - k'| \geq N^{\frac{3}{4}}$  the entries of the inverse matrix must exhibit Gevrey-type decay:

$$|\partial L_N^{-1}(k, k')| \leq \exp \left\{ -\frac{|k - k'|^s}{4} \right\}. \quad (5.3)$$

The inversion result (5.2) follows directly from the inversion condition (3.2) and the derivative identity (5.1). The localization result (5.3) involves basic inequalities associated with Gevrey regularity; the detailed proof is provided in Section C.1. Given that Theorem 3.1 was verified previously, Theorem 5.1 implies the iteration lemma. For technical convenience, we adopt the convention that  $N_{-1} = 0$  and  $\Lambda_{N_{-1}} = \emptyset$ .

**Theorem 5.2** (The Iteration Lemma). Suppose that the tangent frequency satisfies  $\omega_T \in \Omega \setminus (\Omega_M^T \cup G)$ . Let  $\varepsilon_0 = \varepsilon_0(H_1, \Omega, a) > 0$  be the threshold provided in Theorem 1.1. For any  $0 < \varepsilon \leq \varepsilon_0$ , there exists a Gevrey exponent  $s(\varepsilon) > 0$  such that, at the  $r$ -th iteration, the approximate solution  $\hat{z}^{(r)}$  is supported on:

$$\text{supp } \hat{z}^{(r)} \subseteq \Lambda_{N_r}. \quad (5.4)$$

For any index  $i \in \{0, 1, \dots, r\}$  and any  $k \in \Lambda_{N_i} \setminus \Lambda_{N_{i-1}}$ , assume the Gevrey decay property holds:

$$\|\hat{z}^{(r)}(k)\| \leq \sum_{\ell=i}^r \exp \left\{ -\frac{3}{2} N_\ell^s \right\}, \quad (5.5)$$

and the vector field  $F$  satisfies:

$$\|F(\hat{z}_p^{(r)}, \omega_T^{(r+1)}; a, \omega)\| \leq \exp \{-2N_r^s\}. \quad (5.6)$$

Under the numerical update scheme (1.18), these properties are preserved at the  $(r+1)$ -th iteration. Specifically, the update iterate  $\hat{z}^{(r+1)}$  satisfies:

$$\text{supp } \hat{z}^{(r+1)} \subseteq \Lambda_{N_{r+1}}. \quad (5.7)$$

For any  $i \in \{0, 1, \dots, r+1\}$  and any  $k \in \Lambda_{N_i} \setminus \Lambda_{N_{i-1}}$ , the following decay property holds:

$$\|\hat{z}^{(r+1)}(k)\| \leq \sum_{\ell=i}^{r+1} \exp \left\{ -\frac{3}{2} N_\ell^s \right\}, \quad (5.8)$$

and the updated vector field  $F$  satisfies:

$$\|F(\hat{z}_p^{(r+1)}, \omega_T^{(r+2)}; a, \omega)\| \leq \exp \{-2N_{r+1}^s\}. \quad (5.9)$$

*Proof of Theorem 5.2.* For conciseness, we suppress the auxiliary parameters from the dimension-enlarged Newton scheme (1.18b) and define the iterative update as:

$$\Delta^{(r)} = \hat{z}_p^{(r+1)} - \hat{z}_p^{(r)} = -L_{N_{r+1}}^{-1}(\hat{z}_p^{(r)})F(\hat{z}_p^{(r)}). \quad (5.10)$$

The proof is organized in the following three steps.

**Support enlargement** This step verifies the inclusion property (5.7). Given that the perturbation  $H_1$  is a polynomial of total degree at most  $d$ , the vector field is located in the support:

$$\text{supp } F(\hat{z}_p^{(r)}) \subseteq [-dN_r, dN_r]^m \subseteq \left[ -\frac{N_{r+1}}{4}, \frac{N_{r+1}}{4} \right]^m, \quad (5.11)$$

which confirms (5.7) in accordance with the update rule (1.18).

**Lattice vector decay** This step establishes the bound (5.8). Given the inversion condition (3.2) and the previous vector field estimate (5.6), we bound the iterative difference as:

$$\|\Delta^{(r)}\|_2 \leq \|L_{N_{r+1}}^{-1}(\hat{z}_p^{(r)})\|_2 \|F(\hat{z}_p^{(r)})\|_2 \leq \frac{1}{\varepsilon_{N_{r+1}}} \exp\{-2N_r^s\}.$$

Furthermore, by applying Theorem 5.1, we estimate the derivative of the update as:

$$\begin{aligned} \|\partial\Delta^{(r)}\|_2 &\leq \|\partial L_{N_{r+1}}^{-1}(\hat{z}_p^{(r)})\|_2 \|F(\hat{z}_p^{(r)})\|_2 + \|L_{N_{r+1}}^{-1}(\hat{z}_p^{(r)})\|_2 \|\partial F(\hat{z}_p^{(r)})\|_2 \\ &\leq \left( \frac{4\sqrt{m}N_{r+1} + \varepsilon_{N_{r+1}}}{\varepsilon_{N_{r+1}}^2} \right) \exp\{-2N_r^s\}. \end{aligned}$$

By combining the two bounds above, there exists a threshold  $\varepsilon_0 > 0$  such that such that:

$$\|\Delta^{(r)}\| \leq \exp\left\{-\frac{7N_r^s}{4}\right\}, \quad (5.12)$$

for any  $0 < \varepsilon \leq \varepsilon_0$ . We now choose  $s = s(\varepsilon) > 0$  such that  $6M^s \leq 7$ . Consequently, at the  $(r+1)$ -th iteration, for any index  $i \in \{0, 1, \dots, r+1\}$  and any  $k \in \Lambda_{M^i} \setminus \Lambda_{M^{i-1}}$ , the following holds:

$$\|\hat{z}^{(r+1)}(k)\| \leq \|\hat{z}^{(r)}(k)\| + \|\Delta^{(r)}(k)\| \leq \sum_{\ell=i}^{r+1} \exp\left\{-\frac{3}{2}N_\ell^s\right\},$$

which confirms that the decay property (5.8) is preserved across successive iterations.

**Super-exponential convergence** To establish the super-convergence property (5.9), we analyze the behavior of the vector field following the numerical update. By applying a Taylor expansion to the vector field and the frequency, and invoking Theorem 2.3, the post-update residual is bounded by the truncation error and the quadratic terms of the iteration:

$$\|F(\hat{z}_p^{(r+1)}, \omega_T^{(r+2)})\|_2 \leq \|[L - L_{N_{r+1}}]\Delta^{(r)}\|_2 + (2N_{r+1} + 1)^{\frac{m}{2}} \exp\{-3N_{r+1}^s\}. \quad (5.13)$$

Similarly, the derivative of the residual satisfies:

$$\begin{aligned} \|\partial F(\hat{z}_p^{(r+1)}, \omega_T^{(r+2)})\|_2 &\leq \|\partial[L - L_{N_{r+1}}]\Delta^{(r)}\|_2 + \|[L - L_{N_{r+1}}]\partial\Delta^{(r)}\|_2 \\ &\quad + 3(2N_{r+1} + 1)^{\frac{m}{2}} \exp\{-3N_{r+1}^s\}. \end{aligned} \quad (5.14)$$

To estimate the Gevrey norms in (5.13) and (5.14), we exploit the off-diagonal decay of the operators  $L$  and  $L_{N_{r+1}}^{-1}$  established in Theorem 2.2 and Theorem 5.1. Since the estimation procedures for

these terms are analogous, we focus on  $[L - L_{N_{r+1}}]\Delta^{(r)}$  as the representative example. We utilize the following decomposition:

$$\begin{aligned} [L - L_{N_{r+1}}]\Delta^{(r)} &= [(E - P_{N_{r+1}})LP_{N_{r+1}}] \left[ (E - P_{N_{r+1}/3})\Delta^{(r)} \right] \\ &\quad + [(E - P_{N_{r+1}})LP_{N_{r+1}/3}] \Delta^{(r)}. \end{aligned} \quad (5.15)$$

Given the confirmed off-diagonal decay, there exists a threshold  $\varepsilon_0 > 0$  such that for  $0 < \varepsilon \leq \varepsilon_0$ , the following estimates holds:

$$\|(E - P_{N_{r+1}})LP_{N_{r+1}/3}\| \leq \frac{1}{3} \exp \left\{ -\frac{7}{12} N_{r+1}^s \right\}, \quad (5.16)$$

and

$$\|(E - P_{N_{r+1}/3})L_{N_{r+1}}^{-1}P_{N_{r+1}/4}\| \leq \frac{1}{3} \exp \left\{ -\frac{1}{48} N_{r+1}^s \right\}. \quad (5.17)$$

Noting that  $\|(E - P_{N_{r+1}})LP_{N_{r+1}}\| \leq \varepsilon\|S + B\| \leq 1$ , we combine the bounds (5.16) and (5.17) with the decomposition in (5.15) to account for the truncation errors in (5.13) and (5.14). For a sufficiently small threshold  $\varepsilon_0 > 0$ , we obtain

$$\|F(\hat{z}_p^{(r+1)}, \omega_T^{(r+2)})\| \leq \frac{2}{3} \exp \left\{ -\left( \frac{2}{M^s} + \frac{1}{48} \right) N_{r+1}^s \right\} + 4(2N_{r+1} + 1)^{\frac{m}{2}} \exp \left\{ -3N_{r+1}^s \right\}. \quad (5.18)$$

By choosing  $s = s(\varepsilon) > 0$  such that  $95M^s \leq 96$ , we arrive at the desired super-convergence bound:

$$\|F(\hat{z}_p^{(r+1)}, \omega_T^{(r+2)})\|_s \leq \exp \left\{ -2N_{r+1}^s \right\}, \quad (5.19)$$

which concludes the proof of the Iteration Lemma (Theorem 5.2).  $\square$

The decay estimates in Theorem 5.2 demonstrate that despite potential fluctuations in individual terms, the cumulative decay remains strictly controlled. For any multi-index  $k \in \Lambda_{N_r} \setminus \Lambda_{N_{r-1}}$ , the series converges as follows:

$$\sum_{\ell=r}^{\infty} \exp \left\{ -\frac{3N_{\ell}^s}{2} \right\} \leq \exp \left\{ -N_r^s \right\} \leq \exp \left\{ -|k|^s \right\},$$

which ensures that the sequence  $\hat{z}^{(r)}$  remains within the space  $\mathcal{K}(s)$ . Consequently, the solution preserves its spatial localization throughout the iteration, preventing any degradation of regularity as the lattice size  $N$  increases.

## 5.2 Proof of the main theorem

Since  $\hat{z}_q^{(r)}$  stays fixed throughout the iterations, the estimate (5.12) remains valid when  $\hat{z}_p$  is replaced by  $\hat{z}$ . The displacement between successive iterations is bounded as:

$$\|\hat{z}^{(r+1)} - \hat{z}^{(r)}\| = \|\Delta^{(r)}\| \leq \exp \left\{ -\frac{7}{4} N_r^s \right\} = \exp \left\{ -\frac{7}{4} (M^s)^r \right\},$$

which implies the convergence of the sequences  $\{\hat{z}^{(r)}\}$ . Furthermore, we can bound the distance to the limit  $\hat{z}^*$  by estimating the tail of the sequence:

$$\|\hat{z}^{(r)} - \hat{z}^*\| \leq \sum_{\ell=0}^{\infty} \|\hat{z}^{(r+\ell+1)} - \hat{z}^{(r+\ell)}\| \leq \sum_{\ell=0}^{\infty} \exp\left\{-\frac{7}{4}(M^s)^{r+\ell}\right\} \leq \exp\left\{-\frac{3}{2}(M^s)^r\right\},$$

which confirms (1.23a). Moreover, from the tangent frequency update (1.18a) and the uniform bound (2.4b), we have:

$$|\omega_T^{(r+1)} - \omega_T^{(r)}| \leq \varepsilon\gamma \|\hat{z}^{(r+1)} - \hat{z}^{(r)}\| \leq \varepsilon\gamma \exp\left\{-\frac{7}{4}(M^s)^r\right\}.$$

Thus, the convergence of the frequency sequences  $\{\omega_T^{(r)}\}$  is guaranteed, and we also have

$$|\omega_T^{(r)} - \omega_T^*| \leq \sum_{\ell=0}^{\infty} |\omega_T^{(r+\ell+1)} - \omega_T^{(r+\ell)}| \leq \sum_{\ell=0}^{\infty} \varepsilon\gamma \exp\left\{-\frac{7}{4}(M^s)^{r+\ell}\right\} \leq \exp\left\{-\frac{3}{2}(M^s)^r\right\},$$

which confirms (1.23b). Finally, we express the exact solution via its Fourier expansion:

$$z^*(t) = \sum_{k \in \mathbb{Z}^m} \hat{z}^*(k) e^{i\langle k, \omega_T^* \rangle t}.$$

Based on the support property (5.4), the error can be split into two terms:

$$\begin{aligned} \|z^{(r)}(t) - z^*(t)\| &\leq \left\| \sum_{k \in \mathbb{Z}^m} \left( \hat{z}^*(k) - \hat{z}^{(r)}(k) \right) e^{i\langle k, \omega_T^* \rangle t} \right\| + \left\| \sum_{k \in \Lambda_{N_r}} \hat{z}^{(r)}(k) \left( e^{i\langle k, \omega_T^* \rangle t} - e^{i\langle k, \omega_T^{(r)} \rangle t} \right) \right\| \\ &\triangleq I_1 + I_2. \end{aligned}$$

By applying the compact support property (5.4) and the Gevrey decay property (5.5) alongside the Cauchy-Schwarz inequality, we estimate the term  $I_1$  as:

$$\begin{aligned} I_1 &\leq \sum_{k \in \Lambda_{M^r}} \|\hat{z}^*(k) - \hat{z}^{(r)}(k)\| + \sum_{k \notin \Lambda_{M^r}} \|\hat{z}^*(k)\| \\ &\leq \|\hat{z}^{(r)} - \hat{z}^*\| \cdot (2M^r + 1)^{m/2} + \sum_{k \notin \Lambda_{M^r}} e^{-\frac{5}{4}|k|^s} \leq \frac{1}{2} \exp\{-(M^s)^r\}. \end{aligned}$$

where the last inequality follows from the bound (1.23a) established above. Given the uniform boundedness of  $\|\hat{z}^{(r)}\|$ , we again apply the Cauchy-Schwarz inequality to estimate the term  $I_2$  as

$$\begin{aligned} I_2 &\leq \|\hat{z}^{(r)}\| \left( \sum_{k \in \Lambda_{M^r}} \left| e^{i\langle k, \omega_T^* \rangle t} - e^{i\langle k, \omega_T^{(r)} \rangle t} \right|^2 \right)^{\frac{1}{2}} \\ &\leq \left( \|\hat{z}^*\| + \exp\left\{-\frac{3}{2}(M^s)^r\right\} \right) \cdot |\omega_T^{(r)} - \omega_T^*| \cdot \left( \sum_{k \in \Lambda_{M^r}} \|kt\|^2 \right)^{\frac{1}{2}} \leq \frac{1}{2} \exp\{-(M^s)^r\}, \end{aligned}$$

which holds uniformly for any  $t \in [0, N_r] = [0, M^r]$ . By combining the estimate for terms  $I_1$  and  $I_2$ , we arrive at the final time-domain error bound (1.24), which completes the proof of Theorem 1.1.

## 6 Numerical Experiments

Building upon the numerical construction of full-dimensional quasi-periodic solutions developed in [Fu and Shi \[2026\]](#), we extend this framework to the computation of elliptic lower-dimensional quasi-periodic solutions. In contrast to the full-dimensional setting, the lower-dimensional case requires the simultaneous treatment of both the tangent frequencies  $\omega_T$  and the normal frequencies  $\omega_N$ . The latter are of fundamental importance, as they govern the stability and variations of the associated linear quasi-periodic solutions. More specifically, the tangent directions correspond to the excited amplitudes where  $a \neq 0$ , while the normal directions correspond to the non-excited modes where  $a = 0$ .

In this section, we demonstrate the computational efficiency of our alternating numerical procedure [\(1.18\)](#) for constructing such quasi-periodic solutions. Our numerical experiments are conducted on two representative physical models spanning different scales: the macroscopic system from celestial mechanics given by the Hénon-Heiles model, and the microscopic nonlinear lattice system described by the FPU model.

### 6.1 The Hénon-Heiles model

The Hénon-Heiles model serves as a seminal two-degree-of-freedom system, originally developed to describe stellar motion within an axisymmetric galactic potential [[Hénon and Heiles, 1964](#)]. The dynamics of this system evolve within the phase space  $\mathbb{R}^4$ , dictated by the Hamiltonian

$$H = H(x, y) = \frac{1}{2}\omega_1(x_1^2 + y_1^2) + \frac{1}{2}\omega_2(x_2^2 + y_2^2) + \varepsilon \left( y_1^2 y_2 - \frac{y_2^3}{3} \right), \quad (6.1)$$

which is endowed with the canonical symplectic structure  $\varpi = dx \wedge dy$ . To facilitate the implementation of our alternating numerical procedure [\(1.18\)](#), we introduce a complex change of variables for  $j = 1, 2$ , defined as:

$$z_j = \frac{y_j - ix_j}{\sqrt{2}} \quad \text{and} \quad \bar{z}_j = \frac{y_j + ix_j}{\sqrt{2}}.$$

Under this transformation, the Hamiltonian is reformulated as:

$$H = H(z, \bar{z}) = \omega_1 |z_1|^2 + \omega_2 |z_2|^2 + \varepsilon \left[ \frac{1}{2\sqrt{2}}(z_1 + \bar{z}_1)^2(z_2 + \bar{z}_2) - \frac{1}{6\sqrt{2}}(z_2 + \bar{z}_2)^3 \right], \quad (6.2)$$

with the corresponding symplectic structure  $\varpi = idz \wedge d\bar{z}$ .

In the numerical experiments, the perturbation parameter is set to  $\varepsilon = 0.5$ , and the two frequencies are chosen as  $\omega_1 = 1$  and  $\omega_2 = \sqrt{2}$  to satisfy the irrational Diophantine condition. In contrast to the full-dimensional setting where the initial amplitude is typically taken as  $a = (1, 1)$ , we here select the initial amplitudes as  $a = (1, 0)$  and  $a = (0, 1)$  to obtain the lower-dimensional quasi-periodic solutions, with the resulting numerical performance illustrated in [Figure 2](#). It can be observed that when the normal frequency  $\omega_N$  occupies different modes, the system exhibits distinct dynamical behaviors: when the normal frequency satisfies  $\omega_N = \omega_2$ , the tangent mode is perturbed and shifts inward, while the normal mode deviates from the origin to form a perturbed periodic solution; conversely, when the normal frequency satisfies  $\omega_N = \omega_1$ , the tangent mode is also perturbed, manifesting as a rightward protrusion, whereas the normal mode remains localized at the origin. These variations are attributed to the intrinsic asymmetry of the nonlinear perturbation.

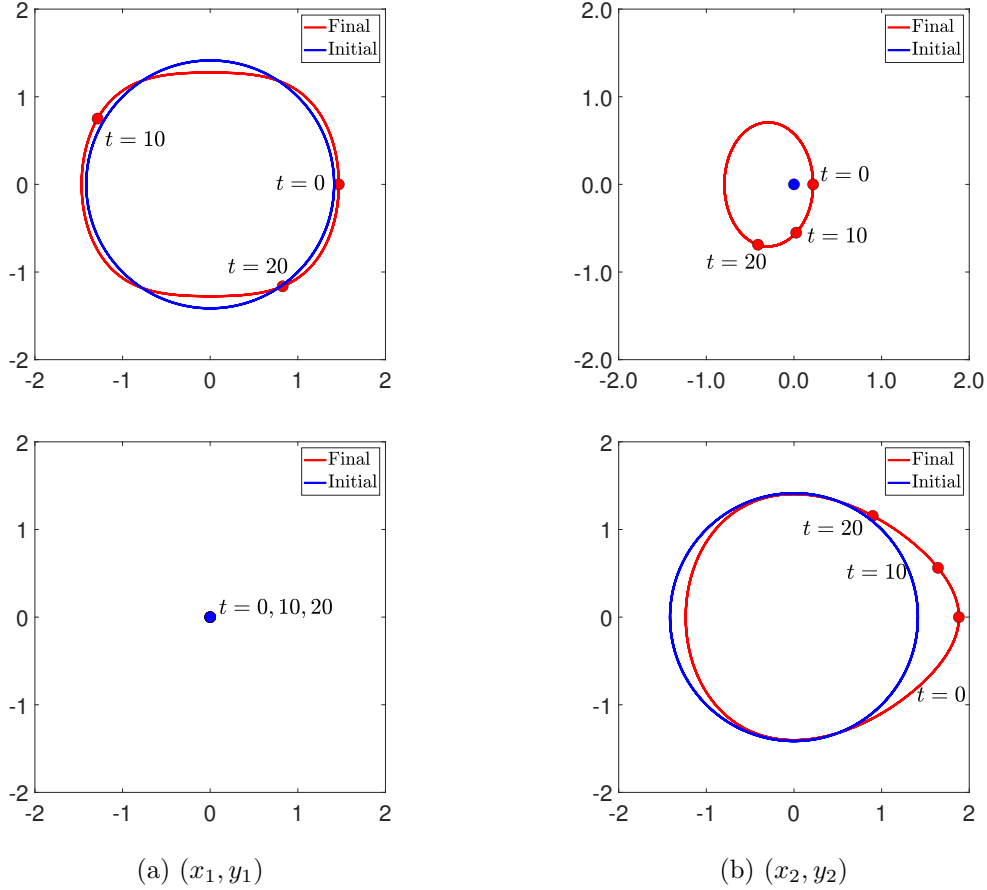


Figure 2: Phase space trajectories of the Hénon-Heiles model with markers indicating specific time points at  $t = 0, 10,$  and  $20,$  where the top and bottom panels correspond to initial amplitudes  $a = (1, 0)$  and  $a = (0, 1),$  respectively.

To further assess the convergence performance, which is consistent with the rigorous statement provided in Theorem 1.1, we examine the iteration errors which exhibit super-exponential convergence as illustrated in Figure 3. Specifically, we track the three key quantities: (i) the Fourier coefficient error,  $\|\hat{z}^{(r+1)} - \hat{z}^{(r)}\|_2,$  measuring the convergence of the coefficients, (ii) the frequency error,  $|\omega^{r+1} - \omega^{(r)}|,$  quantifying the refinement of the computed frequency, and (iii) the point-wise solution error at  $t = 10,$   $|z^{r+1}(10) - z^{(r)}(10)|,$  evaluating the discrepancy of the solution at a fixed time. All three metrics consistently confirm the rapid convergence behavior of the proposed alternating scheme (1.18).

## 6.2 The FPU model

Although the Hénon-Heiles model provides a two-dimensional benchmark, it is important to further validate the effectiveness of the proposed numerical scheme (1.18) in higher-dimensional and more complex systems. For this purpose, we apply this scheme to the Fermi–Pasta–Ulam (FPU) model ( $\beta$ -class), a foundational system in nonlinear physics introduced by Fermi et al. [1965] to investigate

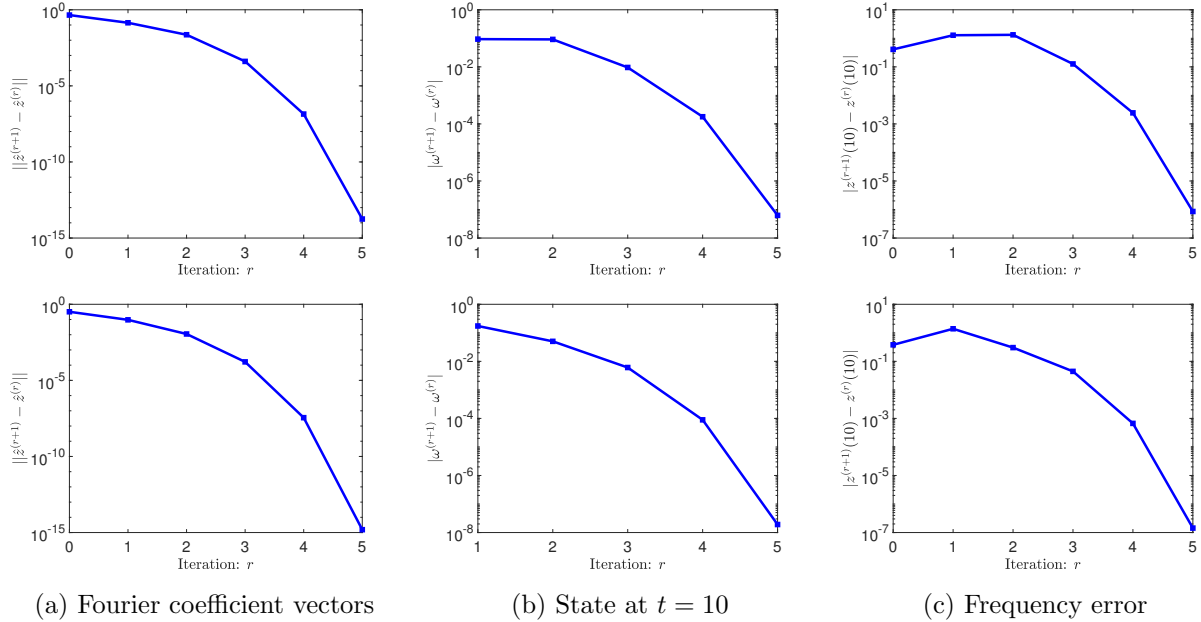


Figure 3: Convergence profiles across iterations for the Hénon-Heiles model, where the top and bottom panels correspond to initial amplitudes  $a = (1, 0)$  and  $a = (0, 1)$ , respectively.

the rate of energy transfer toward equipartition and thermal equilibrium in a vibrating string.

The FPU model describes a one-dimensional chain of  $n$  identical particles of unit mass ( $m = 1$ ) coupled via nonlinear springs. Let  $q = (q_1, \dots, q_n)^\top$  denote the generalized coordinates and  $p = (p_1, \dots, p_n)^\top$  the conjugate momenta. Under the Dirichlet boundary condition ( $q_0 = q_{n+1} = 0$ ), the Hamiltonian is defined on  $\mathbb{R}^{2n}$  as

$$H = \sum_{j=1}^n \frac{p_j^2}{2} + \sum_{j=0}^n \frac{(q_{j+1} - q_j)^2}{2} + \varepsilon \sum_{j=0}^n \frac{(q_{j+1} - q_j)^4}{4}, \quad (6.3)$$

which is endowed with the canonical symplectic structure  $\varpi = dp \wedge dq$ . To facilitate the analysis, we diagonalize the quadratic part via a symmetric orthogonal matrix  $V \in \mathbb{R}^{n \times n}$  with entries:

$$V_{k,j} = \sqrt{\frac{2}{n+1}} \sin\left(\frac{jk\pi}{n+1}\right), \quad j, k = 1, 2, \dots, n.$$

We then perform the canonical transformation  $(p, q) \mapsto (x, y)$  defined by  $x = W^{-1}Vp$  and  $y = WVq$ , where  $W = \text{diag}(\sqrt{\omega_j})$  is a diagonal scaling matrix, and the harmonic frequencies are given by:

$$\omega_k = 2 \sin\left(\frac{k\pi}{2(n+1)}\right), \quad k = 1, 2, \dots, n.$$

Under the defined canonical transformation, the Hamiltonian (6.3) is recast into a more computationally tractable form:

$$H = H(x, y) = \sum_{j=1}^n \frac{\omega_j}{2} (x_j^2 + y_j^2) + \varepsilon H_1(y), \quad (6.4)$$

where the symplectic structure remains invariant ( $\varpi = dx \wedge dy = dp \wedge dq$ ). The quartic perturbation  $H_1(y)$  incorporates the scaling factors and takes the form:

$$H_1(y) = \frac{1}{4} \sum_{j=0}^n \left( \sum_{k=1}^n \frac{V_{j+1,k} - V_{j,k}}{\sqrt{\omega_k}} y_k \right)^4.$$

Finally, following the procedure in (6.1) — (6.2), we transition the Hamiltonian (6.4) into complex coordinates  $z$  and its conjugate  $\bar{z}$  as

$$H = H(z, \bar{z}) = \sum_{j=1}^n \omega_j |z_j|^2 + \varepsilon H_1(z, \bar{z}), \quad (6.5)$$

which is endowed with the symplectic 2-form  $\varpi = idz \wedge d\bar{z}$ . In the complex coordinates, the quartic perturbation is then expressed as

$$H_1(z, \bar{z}) = \frac{1}{4} \sum_{j=0}^n \left( \sum_{k=1}^n \frac{V_{j+1,k} - V_{j,k}}{\sqrt{2\omega_k}} (z_k + \bar{z}_k) \right)^4.$$

With the Hamiltonian formulated in complex variables (6.5), we demonstrate the effectiveness of the proposed alternating numerical procedure (1.18) in capturing the lower-dimensional quasi-periodic solutions within the FPU model. For these numerical trials, we set the system dimension at  $n = 3$ . Unlike the two-dimensional Hénon-Heiles model, which is constrained to a single tangent frequency and one normal frequency, the three-particle FPU model allows us to verify the algorithm's performance across more complex frequency distributions. Specifically, we investigate the following two configurations:

- **Case-I (Periodic solutions):** One tangent frequency and two normal frequencies.
- **Case-II (Quasi-periodic solutions):** Two tangent frequencies and one normal frequency.

The subsequent numerical experiments are divided into two regimes to rigorously evaluate the capture of both one-dimensional and two-dimensional quasi-periodic solutions.

### 6.2.1 Single-frequency periodic solutions

To provide a clear demonstration of the numerical experiments, we set the perturbation parameter to  $\varepsilon = 1$ . The resulting dynamics, depicted in Figure 4, demonstrate that the interaction between two normal frequencies produces behavior significantly more complex than those observed in the Hénon-Heiles model (see Figure 2). The dynamical evolution depends heavily on which mode is selected for the tangent frequency. Specifically, when the tangent frequency is fixed to either the first or third mode (located near the boundary), one normal mode undergoes significant perturbation while the other remains minimally affected. In the two instances, the two normal modes exhibit distinct motion behaviors. Conversely, when the tangent frequency is assigned to the second mode (situated in the middle), both normal modes experience only marginal perturbations. Overall, the coupling of these two normal frequencies fosters more chaotic long-term dynamics, increasing the complexity of the system's quasi-periodic behavior.

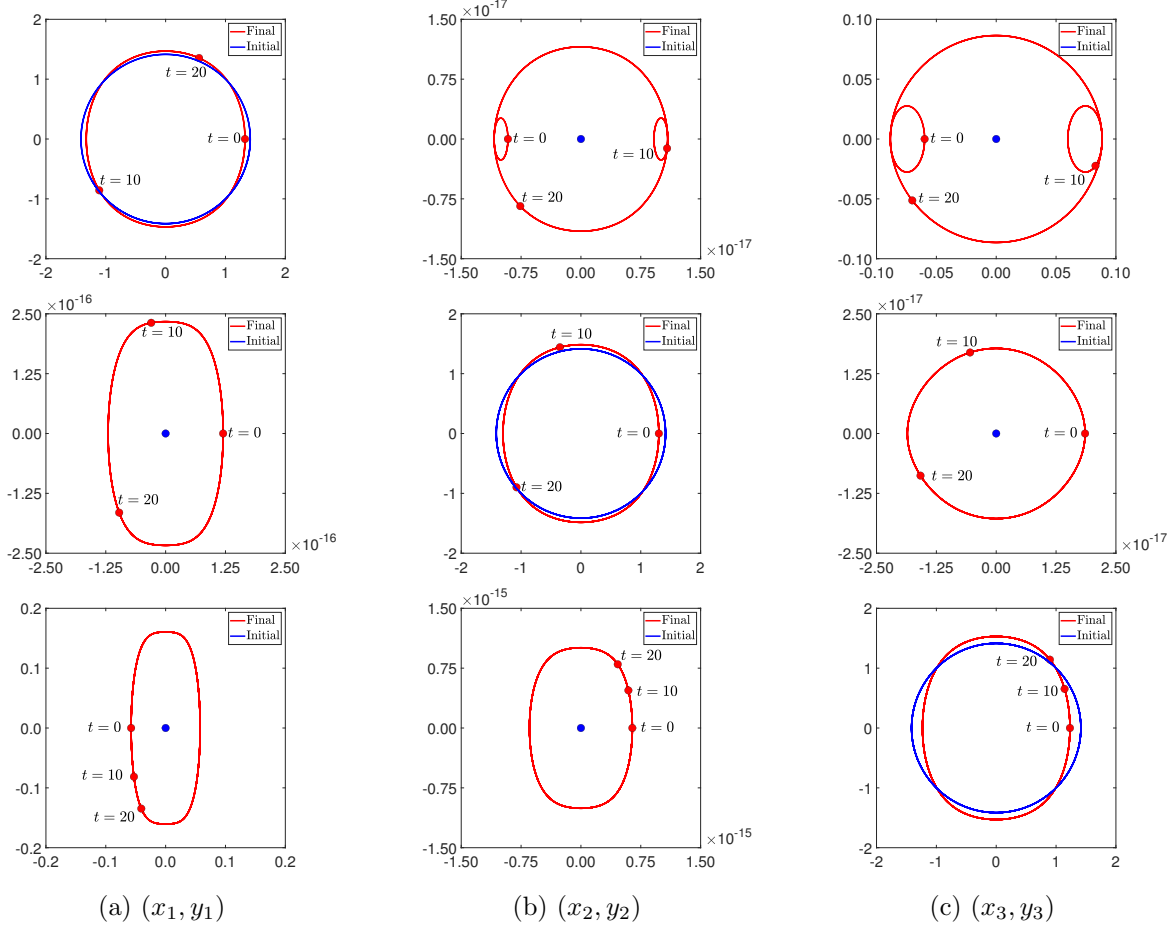


Figure 4: Phase space trajectories of the FPU model with markers indicating specific time points at  $t = 0, 10,$  and  $20$ . The panels represent different initial conditions: (top)  $a = (1, 0, 0)$ ; (middle)  $a = (0, 1, 0)$ ; (bottom)  $a = (0, 0, 1)$ .

The convergence performance for the three cases is illustrated in Figure 5. To evaluate the efficiency of the proposed alternating scheme (1.18), we also monitor the three metrics: the Fourier coefficient error  $\|\hat{z}^{(r+1)} - \hat{z}^{(r)}\|_2$ , the frequency error  $|\omega^{r+1} - \omega^{(r)}|$ , and the pointwise solution error at  $t = 10$ ,  $|z^{r+1}(10) - z^{(r)}(10)|$ . As illustrated, all three indicators consistently exhibit super-exponential decay. This rapid convergence not only validates the theoretical efficiency of the iterative scheme but also highlights its practical utility in achieving high-precision results while bypassing the cumulative phase errors associated with symplectic integrators.

### 6.2.2 Multi-frequency quasi-periodic solutions

In this section, we extend the alternating numerical procedure (1.18) to compute multi-frequency quasi-periodic solutions. By setting  $\varepsilon = 0.1$ , we enhance the visibility of the trajectories within the phase space. Unlike the periodic solutions depicted in Figure 2 and Figure 4, which appear as perfectly closed curves in phase space, the trajectories in Figure 6 characterize quasi-periodic motion. Although these higher-dimensional trajectories never return to their exact starting states,

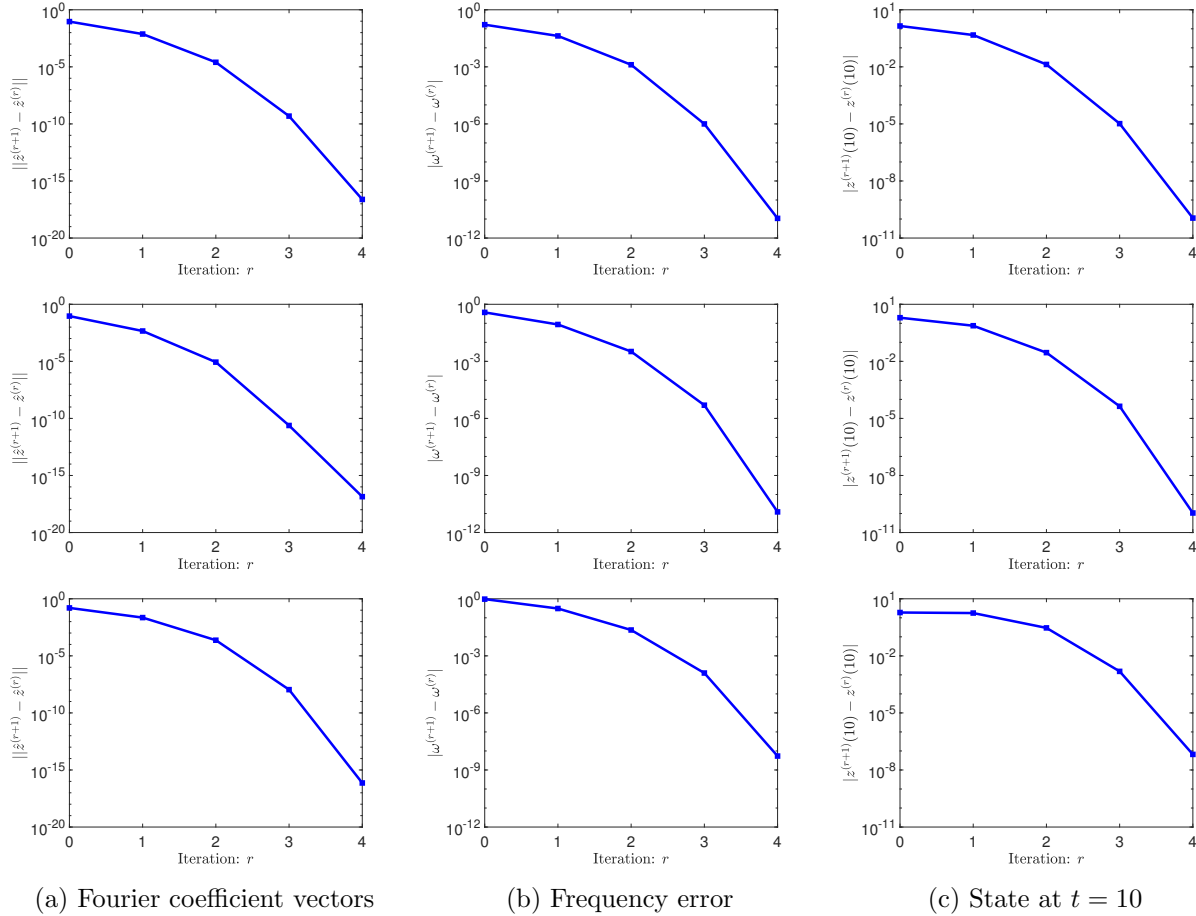


Figure 5: Convergence profiles across iterations for the FPU model. The panels represent different initial conditions: (top)  $a = (1, 0, 0)$ ; (middle)  $a = (0, 1, 0)$ ; (bottom)  $a = (0, 0, 1)$ .

they remain densely confined within the immediate vicinity of their linear unperturbed counterparts, providing visual evidence of the persistence and nonlinear stability of the underlying invariant structures. A notable distinction emerges between the tangential and normal subspaces: while the macroscopic geometric features in the tangential subspaces remain nearly invariant across different active frequencies, indicating a degree of robustness in the dominant dynamics, the microscopic residual fluctuations in the normal subspaces display markedly different geometric patterns. This pronounced variation in the transverse directions suggests the presence of potentially unexplored mathematical or physical mechanisms.

## 7 Conclusion and further work

In this study, we extend the alternating numerical procedure, originally proposed by [Fu and Shi \[2026\]](#), to investigate elliptic lower-dimensional quasi-periodic solutions. By conducting a comparative analysis of two Newton-based iterative methods, the KAM scheme and the CWB scheme, we identify a potentially deeper underlying structure governing the quasi-periodic solutions of nearly

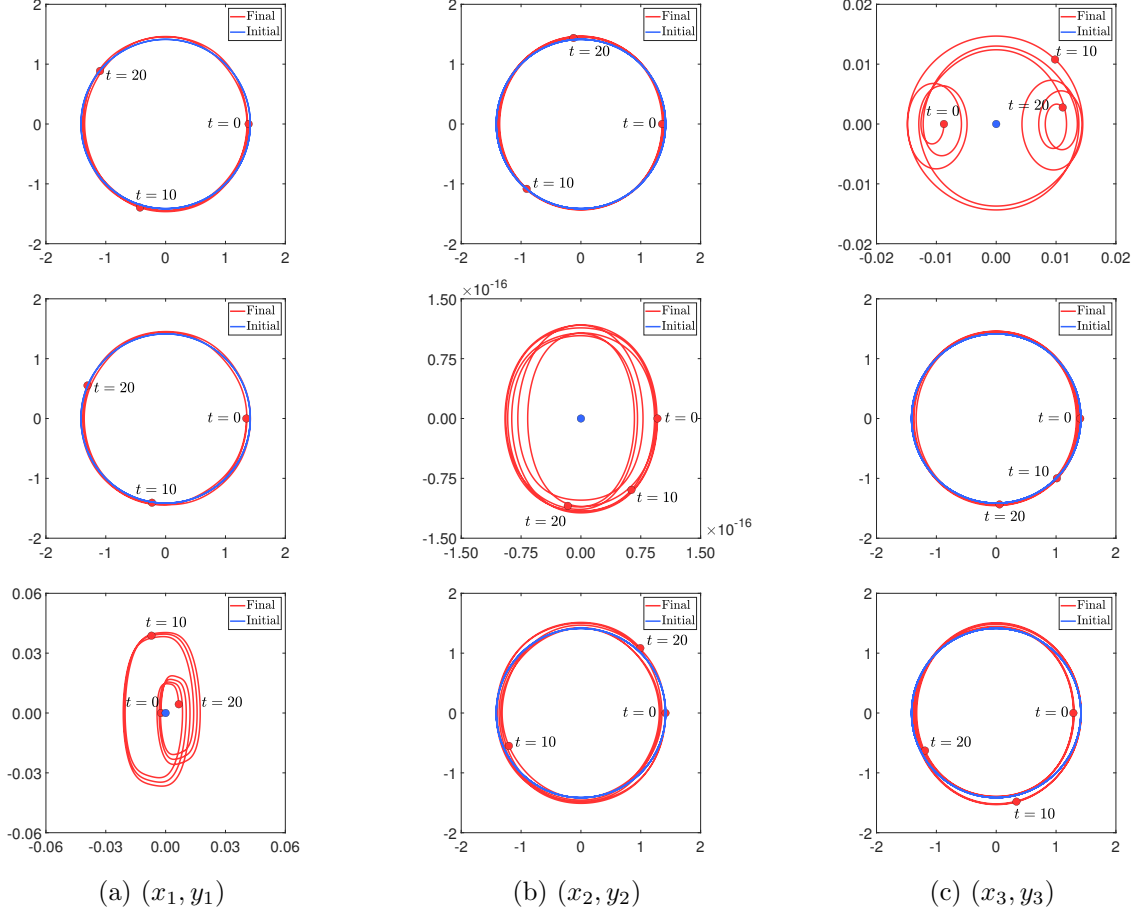


Figure 6: Phase space trajectories of the FPU model with markers indicating specific time points at  $t = 0, 10,$  and  $20$ . The panels represent different initial conditions: (top)  $a = (1, 1, 0)$ ; (middle)  $a = (1, 0, 1)$ ; (bottom)  $a = (0, 1, 1)$ .

integrable systems. For clarity and conciseness, we employ the full-dimensional case as an illustrative example. In an integrable system, quasi-periodic solutions are represented by the linear solution (1.1). The KAM scheme operates by subtracting this entire linear component from the total solution, effectively isolating the perturbation from the unperturbed torus  $\{0\} \times \mathbb{T}^n$  associated with the Hamiltonian (1.2). Under the assumption that this perturbation contains no linear terms, the resulting solution is defined relative to the frequency  $\omega(I_0)$ , simplified as  $\omega$ . Consequently, the total quasi-periodic solution in complex coordinates is reconstructed as:

$$z(t) = \underbrace{\sum_{j=1}^n \sqrt{I_{0,j}} e^{i\omega_j t}}_{\text{Linear part}} + \underbrace{f(\omega t)}_{\text{Perturbation}}. \quad (7.1)$$

In contrast, within the CWB scheme, the linear solution cannot be treated as the full initial condition. Instead, it must be considered as:

$$I(t) = I_0 - a^2, \quad \theta(t) = \omega(I_0 - a^2)t + \theta_0,$$

where  $a^2 = (a_1^2, \dots, a_n^2)^\top \neq 0$ . The Hamiltonian for the perturbation solution becomes:

$$H = \langle \omega(I_0 - a^2), J + a^2 \rangle + \varepsilon H_1(J + a^2, \theta; I_0 - a^2).$$

Accordingly, the resulting quasi-periodic solution takes the form

$$z(t) = \sum_{j=1}^n \sqrt{I_{0,j} - a_j^2} e^{i\omega_j(I_0 - a^2)t} + \sum_{j=1}^n a_j \left( e^{i\omega'_j(I_0 - a^2)t} - e^{i\omega_j(I_0 - a^2)t} \right) + \sum_{k \notin S} \hat{z}_k e^{i\langle k, \omega'(I_0 - a^2) \rangle t}. \quad (7.2)$$

Intuitively, as the parameter  $|a| \rightarrow 0$ , the frequencies should satisfy  $\omega(I_0 - a^2) \rightarrow \omega$  and  $\omega'(I_0 - a^2) \rightarrow \omega$ . If this convergence is rigorously established, the quasi-periodic solution from the CWB scheme (7.2) admits the simplified representation

$$z(t) = \underbrace{\sum_{j=1}^n \sqrt{I_{0,j}} e^{i\omega_j t}}_{\text{Linear part}} + \underbrace{\sum_{k \notin S} \hat{z}_k e^{i\langle k, \omega \rangle t}}_{\text{Perturbation}}. \quad (7.3)$$

Comparing (7.1) and (7.3), we can derive that the perturbation is given by

$$f(\omega t) = \sum_{k \notin S} \hat{z}_k e^{i\langle k, \omega \rangle t},$$

which reveals that the perturbation involves only the coefficients of the non-resonant Fourier modes. Furthermore, as we transition from an integrable system to a nearly integrable one, the quasi-periodic solution evolves from a simple linear mode superposition into a complex periodic function of  $\theta = \omega t$ . An interesting direction for future research is to investigate the behavior of the coefficients of non-resonant Fourier modes across different perturbation Hamiltonians.

In the forthcoming work, we plan to demonstrate the application of our alternating numerical scheme to construct quasi-periodic solutions for nearly integrable systems involving infinite normal frequencies. Specifically, we first address the infinite-dimensional FPU model and weakly coupled lattice networks, as discussed by Aubry [1997], for which the existence of invariant tori was established via the KAM technique by Yuan [2002]. We then extend our investigation to nearly integrable systems governed by nonlinear partial differential equations (PDEs), including the nonlinear Schrödinger (NLS), nonlinear wave (NLW), and KdV equations [Kuksin, 2000, Kappeler and Pöschel, 2003]. Furthermore, we aim to present several previously undiscovered exact solutions, specifically for the NLS. It is also worth noting that for the NLS equation in higher spatial dimensions, a class of special  $d$ -dimensional quasi-periodic solutions was constructed via the KAM technique by Yuan [2003].

## Acknowledgements

This work was partially supported by the NSFC (Grant No. 12241105) and by SIMIS (startup fund and cross-disciplinary research projects).

## References

- V. I. Arnold. Proof of a theorem of A. N. Kolmogorov on the invariance of quasi-periodic motions under small perturbations of the Hamiltonian. *Russian Mathematical Surveys*, 18(5):9–36, 1963.
- V. I. Arnold. Instability of dynamical systems with several degrees of freedom. *Soviet Mathematics*, 5:581–585, 1964.
- V. I. Arnold. *Mathematical methods of classical mechanics*, volume 60. Springer Science & Business Media, 2013.
- S. Aubry. Breathers in nonlinear lattices: Existence, linear stability and quantization. *Physica D: Nonlinear Phenomena*, 103(1-4):201–250, 1997.
- J. Bourgain. On Melnikov’s persistence problem. *Mathematical Research Letters*, 4(4):445–458, 1997.
- J. Bourgain. *Green’s Function Estimates for Lattice Schrödinger Operators and Applications*. Princeton University Press, Princeton, 2005.
- L. H. Eliasson. Perturbations of stable invariant tori for Hamiltonian systems. *Annali della Scuola Normale Superiore di Pisa-Classe di Scienze*, 15(1):115–147, 1988.
- K. Feng. *Collected Works of Feng Kang*, volume II. Science Press, Beijing, 1995. Edited by Institute of Computational Mathematics and Scientific/Engineering Computing, Academy of Mathematics and Systems Science, Chinese Academy of Sciences; Proofread by Liqun, Cao and Yifa, Tang.
- E. Fermi, J. Pasta, and S. Ulam. Studies of nonlinear problems I. In *Collected Papers of Enrico Fermi*. University of Chicago Press, 1965. Originally published as Los Alamos report LA-1940, 1955.
- M. Fu and B. Shi. Numerical construction of quasi-periodic solutions beyond symplectic integrators. *arXiv preprint arXiv:2602.16275*, 2026.
- L. Gauckler, E. Hairer, and C. Lubich. Dynamics, numerical analysis, and some geometry. In *Proceedings of the International Congress of Mathematicians: Rio de Janeiro 2018*, pages 453–485. World Scientific, 2018.
- E. Hairer, C. Lubich, and G. Wanner. *Geometric Numerical Integration: Structure-Preserving Algorithms for Ordinary Differential Equations*, volume 31 of *Springer Series in Computational Mathematics*. Springer Berlin Heidelberg, second edition, 2006.
- M. Hénon and C. Heiles. The applicability of the third integral of motion: some numerical experiments. *Astronomical Journal*, 69:73–79, 1964.
- T. Kappeler and J. Pöschel. *KdV & KAM*. Ergebnisse der Mathematik und ihrer Grenzgebiete. 3. Folge / A Series of Modern Surveys in Mathematics. Springer Berlin, Heidelberg, 1 edition, 2003.
- A. N. Kolmogorov. On the preservation of conditionally periodic motions under a small change of the Hamiltonian function. *Doklady Akademii Nauk SSSR*, 98:527–530, 1954. (in Russian); English translation in *Lecture Notes in Physics* **93** (1979), 51–56.

- S. B. Kuksin. *Analysis of Hamiltonian PDEs*, volume 19. Clarendon Press, 2000.
- B. Y. Levin. *Lectures on entire functions*, volume 150. American Mathematical Society, 1996.
- V. K. Melnikov. On certain cases of conservation of almost periodic motions with a small change of the Hamiltonian function. In *Doklady Akademii Nauk*, volume 165, pages 1245–1248. Russian Academy of Sciences, 1965.
- V. K. Melnikov. A certain family of conditionally periodic solutions of a hamiltonian system. *Doklady Akademii Nauk SSSR*, 181:546–549, 1968.
- J. Moser. On the theory of quasiperiodic motions. *SIAM Review*, 8(2):145–172, 1966.
- J. Moser. Convergent series expansions for quasi-periodic motions. *Mathematische Annalen*, 169(1):136–176, 1967.
- J. K. Moser. On invariant curves of area-preserving mapping of an annulus. *Nachrichten der Akademie der Wissenschaften in Göttingen, II*, pages 1–20, 1962.
- J. Pöschel. On elliptic lower dimensional tori in Hamiltonian systems. *Mathematische Zeitschrift*, 202(4):559–608, 1989.
- J. Pöschel. A lecture on the classical KAM theorem. In *Proceedings of Symposia in Pure Mathematics*, volume 69, pages 707–732, Providence, RI, 2001. American Mathematical Society.
- X. Yuan. Construction of quasi-periodic breathers via KAM technique. *Communications in Mathematical Physics*, 226(1):61–100, 2002.
- X. Yuan. Quasi-periodic solutions of nonlinear schrödinger equations of higher dimension. *Journal of Differential Equations*, 195(1):230–242, 2003.

## A Proofs of results in Section 2

In this appendix, we provide detailed proofs for the results in Section 2, especially for Theorem 2.1 — Theorem 2.4 (see Section A.2 — Section A.5). To facilitate these proofs, we first establish an elementary inequality and show that the Gevrey decay property is preserved under convolution. These preliminary results are rigorously stated in the following lemmas.

### A.1 Preliminary lemmas

**Lemma A.1.** Let  $a, b \geq 0$  and  $0 < s < 1$ . Then the following inequality holds:

$$a^s + b^s - (a + b)^s \geq (2 - 2^s) \min\{a, b\}^s. \quad (\text{A.1})$$

*Proof.* Without loss of generality, we assume  $a \geq b$ . The case  $b = 0$  is trivial, so we consider  $b > 0$ . Define  $x = a/b \geq 1$  and consider the function  $f(x) = x^s + 1 - (1 + x)^s$ . Since  $0 < s < 1$ , its derivative satisfies  $f'(x) = s(x^{s-1} - (x + 1)^{s-1}) > 0$  for all  $x \geq 1$ . Thus,  $f$  is strictly increasing on  $[1, \infty)$ , which implies  $f \geq f(1) = 2 - 2^s$ . Taking  $x = a/b$ , we derive the inequality (A.1), so the proof is complete.  $\square$

Next, we use Theorem A.1 to show that the Gevrey decay property is preserved under convolution.

**Lemma A.2.** Let the Gevrey decay set  $\mathcal{K}(s)$  be defined in (1.22). For any  $\hat{a}, \hat{b} \in \mathcal{K}(s)$ , there exists a constant  $C_2(m, s) > 0$  such that their convolution satisfies

$$\sup_{k \in \mathbb{Z}^m} \left( |(\hat{a} * \hat{b})(k)| \exp \{|k|^s\} \right) \leq C_2(m, s). \quad (\text{A.2})$$

More generally, if  $\hat{a}_j(k) \in \mathcal{K}(s)$  for  $j = 1, \dots, \ell$ , then there exists a constant  $C_\ell(m, s) > 0$  such that the  $\ell$ -fold convolution satisfies:

$$\sup_{k \in \mathbb{Z}^m} \left( |(\hat{a}_1 * \hat{a}_2 * \dots * \hat{a}_\ell)(k)| \exp \{|k|^s\} \right) \leq C_\ell(m, s). \quad (\text{A.3})$$

*Proof.* Given that  $\hat{a}, \hat{b} \in \mathcal{K}(s)$ , we estimate their convolution as

$$\begin{aligned} |(\hat{a} * \hat{b})(k)| &\leq \sum_{k' \in \mathbb{Z}^m} |\hat{a}(k - k')| |\hat{b}(k')| \\ &\leq \sum_{k' \in \mathbb{Z}^m} \exp \{-|k - k'|^s\} \exp \{-|k'|^s\} \\ &\leq \sum_{k' \in \mathbb{Z}^m} \exp \{-|k|^s\} \exp \left\{ -(|k - k'|^s + |k'|^s - (|k - k'| + |k'|)^s) \right\}, \end{aligned}$$

where the last step uses the triangle inequality. Applying Theorem A.1 to bound the sum involving the remaining exponential terms, we have

$$|(\hat{a} * \hat{b})(k)| \leq \exp \{-|k|^s\} \left( \sum_{k' \in \mathbb{Z}^m} \exp \left\{ -(2 - 2^s) \min \{|k - k'|^s, |k'|^s\} \right\} \right).$$

Since the sum of the Gevrey decay series converges in an  $m$ -dimensional lattice  $\mathbb{Z}^m$ , we establish the inequality (A.2). By induction, this same argument extends to any finite  $\ell$ -fold convolutional product, thereby establishing the inequality (A.3).  $\square$

## A.2 Proof of Theorem 2.1

Since the perturbation  $H_1$  is a polynomial with real coefficients, each component of its associated vector field,  $\partial H_1 / \partial \bar{z}_j$  for  $j = 1, \dots, n$ , is likewise a real-coefficient polynomial. Given that  $\hat{z} \in \mathcal{K}(s)$ , Theorem A.2 implies that the Fourier coefficients  $\hat{X}(k)$  exhibit Gevrey decay. By applying the Leibniz rule, it follows that the derivative  $\partial_{\omega_T} \hat{X}(k)$  also exhibits Gevrey decay, which leads directly to the estimate provided in (2.3a). By summing these Gevrey decay series, we derive a uniform bound for the vector field as expressed in (2.3b). This concludes the proof.

## A.3 Proof of Theorem 2.2

We begin by considering the full tangent operator, denoted as  $\mathcal{H} = \partial \hat{X} / \partial \hat{z}$ . For any  $k, k' \in \mathbb{Z}^m$ , its component is given by

$$\mathcal{H}(k - k') = \frac{2}{(2\pi)^m} \int_{\mathbb{T}^m} \frac{\partial^2 H_1}{\partial z \partial \bar{z}} \cos(\langle k - k', \theta \rangle) d\theta.$$

Following a similar argument to that used for the vector field, we apply Theorem A.2 to derive uniform bounds for  $\mathcal{H}$  across the full lattice  $\mathbb{Z}^m$ . Since  $S$  represents this operator restricted specifically to non-resonant indices, the uniform bound naturally extends directly to  $S$ , thereby verifying the inequality (2.4a).

To bound the operator norm of  $\mathcal{H}$ , we evaluate the norm of  $\mathcal{H}\hat{z}$  for any  $\hat{z} \in \ell_2$  as

$$\begin{aligned} \|\mathcal{H}\hat{z}\|^2 &= \sum_{k \in \mathbb{Z}^m} \left\| \sum_{k' \in \mathbb{Z}^m} \mathcal{H}(k') \hat{z}(k - k') \right\|^2 \\ &\leq \sum_{k \in \mathbb{Z}^m} \left( \sum_{k' \in \mathbb{Z}^m} \|\mathcal{H}(k')\|^{\frac{1}{2}} \cdot \|\mathcal{H}(k')\|^{\frac{1}{2}} \|\hat{z}(k - k')\| \right)^2. \end{aligned}$$

Given that the operator  $\mathcal{H}$  exhibits Gevrey decay, we apply the Cauchy-Schwarz inequality to establish the following bound

$$\|\mathcal{H}\hat{z}\|^2 \leq \left[ \sum_{k \in \mathbb{Z}^m} \|\mathcal{H}(k)\| \right]^2 \left[ \sum_{k \in \mathbb{Z}^m} \|\hat{z}(k)\|^2 \right] < \infty. \quad (\text{A.4})$$

Note that these operators,  $\partial \hat{X}_q / \partial \hat{z}_p$ ,  $S$ , and  $\partial \hat{X} / \partial \hat{z}$ , are the full tangent operator  $\partial \hat{X} / \partial \hat{z}$  restricted to specific index sets. Since the  $\ell_2$ -norm of a restricted operator is bounded by that of the full operator, we arrive at the inequality (2.4b), which completes the proof.

#### A.4 Proof of Theorem 2.3

Following the same procedure used for vector fields and tangent operators, we analyze the third-order tensor  $\partial^2 \hat{X} / \partial \hat{z}^2$ . For any  $k, k', k'' \in \mathbb{Z}^m$ , we derive the kernels as

$$\begin{aligned} \frac{\partial^2 \hat{X}(k)}{\partial \hat{z}(k') \partial \hat{z}(k'')} &= \mathcal{T}_{11}(k - k' - k'') + \mathcal{T}_{21}(k + k' - k'') + \mathcal{T}_{12}(k - k' + k'') + \mathcal{T}_{22}(k + k' + k'') \\ &= \frac{1}{(2\pi)^m} \int_{\mathbb{T}^m} \frac{\partial^3 H_1}{\partial z^2 \partial \bar{z}} e^{-i\langle k - k' - k'', \theta \rangle} d\theta + \frac{1}{(2\pi)^m} \int_{\mathbb{T}^m} \frac{\partial^3 H_1}{\partial z \partial \bar{z}^2} e^{-i\langle k + k' - k'', \theta \rangle} d\theta \\ &\quad + \frac{1}{(2\pi)^m} \int_{\mathbb{T}^m} \frac{\partial^3 H_1}{\partial z \partial \bar{z}^2} e^{-i\langle k - k' + k'', \theta \rangle} d\theta + \frac{1}{(2\pi)^m} \int_{\mathbb{T}^m} \frac{\partial^3 H_1}{\partial z^2 \partial \bar{z}} e^{-i\langle k + k' + k'', \theta \rangle} d\theta. \end{aligned}$$

Given that  $\hat{z} \in \mathcal{K}(s)$  and the perturbation  $H_1$  is a real-coefficient polynomial, there exists some constant  $\gamma_8 = \gamma_8(H_1, s) > 0$  such that

$$\sup_{k, k', k'' \in \mathbb{Z}^m} \left( \|\mathcal{T}_{ij}(k + (-1)^i k' + (-1)^j k'')\| \exp \{ |k + (-1)^i k' + (-1)^j k''|^s \} \right) \leq \gamma_8,$$

which demonstrates that the tensors  $\mathcal{T}_{ij}$  for  $i, j \in \{1, 2\}$  exhibit Gevrey decay.

To bound the tensors, consider two vectors,  $\hat{z}_1$  and  $\hat{z}_2$ , with support contained within  $\Lambda_N$ . Taking  $\mathcal{T}_{11}$  as a representative example, we apply the Cauchy-Schwarz inequality to derive the following bound as

$$\|\mathcal{T}_{11}(\hat{z}_1, \hat{z}_2)\|^2$$

$$\begin{aligned}
&= \sum_{k \in \mathbb{Z}^m} \left\| \sum_{k'' \in \Lambda_N} \sum_{k' \in \Lambda_N} \mathcal{T}_{11}(k - k' - k'') \hat{z}_1(k') \hat{z}_2(k'') \right\|^2 \\
&\leq \sum_{k \in \mathbb{Z}^m} \left[ \sum_{k', k'' \in \Lambda_N} \|\mathcal{T}_{11}(k - k' - k'')\| \right] \cdot \left[ \sum_{k', k'' \in \Lambda_N} \|\mathcal{T}_{11}(k - k' - k'')\| \|\hat{z}_1(k')\|^2 \|\hat{z}_2(k'')\|^2 \right] \\
&\leq \left[ \sum_{k', k'' \in \Lambda_N} \gamma_8 e^{-|k - k' - k''|^s} \right] \cdot \left[ \sum_{k \in \mathbb{Z}^m} \sum_{k', k'' \in \Lambda_N} \gamma_8 e^{-|k - k' - k''|^s} \|\hat{z}_1(k')\|^2 \|\hat{z}_2(k'')\|^2 \right] \\
&\leq 2\gamma_8^2 (2N + 1)^m \left[ \sum_{k \in \mathbb{Z}^m} e^{-|k|^s} \right] \left[ \sum_{k' \in \Lambda_N} \|\hat{z}_1(k')\|^2 \right] \left[ \sum_{k'' \in \Lambda_N} \|\hat{z}_2(k'')\|^2 \right] \\
&= 2\gamma_8^2 (2N + 1)^m \left[ \sum_{k \in \mathbb{Z}^m} e^{-|k|^s} \right] \cdot \|\hat{z}_1\|^2 \|\hat{z}_2\|^2 < \infty.
\end{aligned}$$

Similarly, we establish the corresponding bounds for  $\mathcal{T}_{21}$ ,  $\mathcal{T}_{12}$ , and  $\mathcal{T}_{22}$ . These operators,  $\partial^2 \hat{X}_q / \partial \hat{z}_p^2$ ,  $\partial \mathcal{S} / \partial \hat{z}_p$ , and  $\partial^2 \hat{X} / \partial \hat{z}_p^2$ , are restrictions of the full tangent operator  $\partial^2 \hat{X} / \partial \hat{z}^2$  to specific index sets. Since the  $\ell_2$ -norm of a restricted operator is bounded by that of the full operator, we arrive at the inequality (2.5), which completes the proof.

### A.5 Proof of Theorem 2.4

Recalling the operator  $B$  defined in (1.19), we observe that for any  $k, k' \notin \mathcal{S}$ , its entries satisfy the following inequality:

$$\|B(k, k')\| \leq \frac{1}{e} \left\| \frac{\partial \langle k, \hat{X}_q \rangle}{\partial \hat{z}_p(k')} \hat{z}_p(k) \right\|.$$

For any  $\hat{z} \in \mathcal{K}(s)$ , we apply the decay properties established in Theorem 2.1 to verify the Gevrey bound in (2.6a). Given that  $B$  is a rank-one operator, we apply the Cauchy-Schwarz inequality to bound its norm as follows:

$$\|B(k, k')\| \leq \frac{1}{e} \|k \hat{z}_p(k)\| \cdot \left\| \frac{\partial \hat{X}_q}{\partial \hat{z}_p(k')} \right\|.$$

By utilizing the Gevrey decay of the tangent operators derived in Section A.3, we extend the bound over the lattice  $\mathbb{Z}^m \times \mathbb{Z}^m$  as

$$\|B\| \leq \sum_{k \in \mathbb{Z}^m} \left( \frac{\|k \hat{z}_p(k)\|}{e} \right) \cdot \sum_{k' \in \mathbb{Z}^m} \left( \left\| \frac{\partial \hat{X}_q}{\partial \hat{z}_p(k')} \right\| \right).$$

Finally, since  $\hat{z} \in \mathcal{K}(s)$ , we invoke Theorem 2.1 and Theorem 2.2 to ensure the convergence of the infinite sum over the lattice, thereby confirming the uniform bound as stated in (2.6b).

## B Proofs of results in Section 3

In this appendix, we provide the detailed proofs for the results presented in Section 3, specifically addressing Theorem 3.2 and Theorem 3.3.

## B.1 Proof of Theorem 3.2

Let  $\Omega \subseteq \mathbb{R}^m$  be a bounded domain, and denote its diameter as  $d = \max_{x,y \in \Omega} \|x - y\|_2$ . For each integer vector  $k \in \mathbb{Z}^m \setminus \{0\}$ , the corresponding nearly-resonant strip is enclosed by two parallel hyperplanes perpendicular to  $k$ . Consequently, the measure of the tangent nearly-resonant sets defined in (3.5) satisfies

$$\text{mes}(\Omega_{0,M}^\tau) \leq \sum_{k \in \mathbb{Z}^m \setminus \{0\}} \frac{2d^{m-1}}{(\|k\|_2)^{\tau+1}}.$$

Similarly, we estimate the measures for the total single-mode resonant set (3.6) and the total difference resonant set (3.7) as

$$\begin{cases} \text{mes}(\Omega_{1,M}^\tau) \leq \sum_{k \in \mathbb{Z}^m} \frac{2(n-m)d^{m-1}}{(\|k\|_2 + 1)^{\tau+1}}, \\ \text{mes}(\Omega_{2,M}^\tau) \leq \sum_{k \in \mathbb{Z}^m} \frac{4(n-m)^2 d^{m-1}}{(\|k\|_2 + 2)^{\tau+1}}. \end{cases}$$

Since the exponent satisfies  $\tau > m - 1$ , the lattice series  $\sum_{k \in \mathbb{Z}^m \setminus \{0\}} \|k\|_2^{-\tau-1}$  converges. By combining the above estimates, we establish the desired bound (3.8), which completes the proof.

## B.2 Proof of Theorem 3.3

Before proceeding to the proof of Theorem 3.3, we establish a lemma regarding the preservation of the Gevrey decay property under operator multiplication. We say that an operator  $A : \ell_2(\mathbb{Z}^m) \mapsto \ell_2(\mathbb{Z}^m)$  exhibits *proper decay* if its entries satisfy:

$$\sup_{k,k' \in \mathbb{Z}^m} (|A(k,k')| \exp\{|k - k'|^s\}) \leq 1.$$

**Lemma B.1.** Let  $A_1$  and  $A_2$  be two operators with proper decay. Then there exists a constant  $C'_2(m,s) > 0$  such that their product  $\mathcal{A} = A_1 A_2$  satisfies

$$\sup_{k,k' \in \mathbb{Z}^m} (|\mathcal{A}(k,k')| \exp\{|k - k'|^s\}) \leq C'_2(m,s). \quad (\text{B.1})$$

More generally, for any finite collection of operators  $\{A_j\}_{j=1}^\ell$  with proper decay, there exists a constant  $C'_\ell(m,s) > 0$  such that the  $\ell$ -fold product  $\mathcal{A} = \prod_{j=1}^\ell A_j$  satisfies:

$$\sup_{k,k' \in \mathbb{Z}^m} (|\mathcal{A}(k,k')| \exp\{|k - k'|^s\}) \leq C'_\ell(m,s). \quad (\text{B.2})$$

*Proof.* Given that  $A_1$  and  $A_2$  possess proper decay, the entries of their product are bounded by:

$$\begin{aligned} |\mathcal{A}(k,k')| &\leq \sum_{k'' \in \mathbb{Z}^m} |A_1(k,k'')| |A_2(k'',k')| \\ &\leq \sum_{k'' \in \mathbb{Z}^m} \exp\{-|k - k''|^s - |k'' - k'|^s\} \\ &\leq \exp\{-|k - k'|^s\} \sum_{k'' \in \mathbb{Z}^m} \exp\{-(2 - 2^s) \min\{|k - k''|^s, |k'' - k'|^s\}\}, \end{aligned}$$

where the last inequality follows from Theorem A.1. Since the Gevrey decay series converges, the summation above is bounded by a constant depending only on  $m$  and  $s$ , thus we establish the inequality (B.1). The general estimate (B.2) follows immediately by induction on  $\ell$ .  $\square$

We now complete the proof of Theorem 3.3. Since the diagonal operator  $D_N$  admits the uniform lower bound (3.11), it is invertible. This allows us to factor the restricted operator  $(T + \varepsilon B)_N$  as follows:

$$(T + \varepsilon B)_N = D_N + \varepsilon(S_N + B_N) = D_N [I + \varepsilon D_N^{-1}(S_N + B_N)].$$

Given the smallness of the perturbation parameter  $\varepsilon$ , the operator  $(T + \varepsilon B)_N$  is invertible, and its inverse can be expanded as the Neumann series:

$$(T + \varepsilon B)_N^{-1} = [I + \varepsilon D_N^{-1}(S_N + B_N)]^{-1} D_N^{-1} = \left\{ \sum_{\ell=0}^{\infty} [-\varepsilon D_N^{-1}(S_N + B_N)]^{\ell} \right\} D_N^{-1}. \quad (\text{B.3})$$

By applying the bound for  $\|D_N^{-1}\|_2$  from (3.11) alongside the estimates from Theorem 2.2 and Theorem 2.4, we derive the following bound

$$\|(T + \varepsilon B)_N^{-1}\|_2 \leq \|D_N^{-1}\|_2 \left( \sum_{\ell=0}^{\infty} \|\varepsilon D_N^{-1}(S_N + B_N)\|_2^{\ell} \right) \leq \frac{1}{\varepsilon_N},$$

which confirms the norm bound (3.9). To establish the off-diagonal decay, we rewrite the Neumann series (B.3) to isolate the higher-order terms:

$$(T + \varepsilon B)_N^{-1} = D_N^{-1} - \left[ \sum_{\ell=0}^{\infty} (-\varepsilon D_N^{-1}(S_N + B_N))^{\ell} \right] (\varepsilon D_N^{-1}(S_N + B_N) D_N^{-1}).$$

Utilizing the Gevrey decay properties for the entries of the operators  $S$  and  $B$  (Theorem 2.2 and Theorem 2.4), Theorem B.1 implies that for any  $k \neq k'$ :

$$\left| (-\varepsilon D_N^{-1}(S_N + B_N))^{\ell}(k, k') \right| \leq \left( \frac{1}{2} \right)^{\ell+1} \exp \{ -|k - k'|^s \}.$$

By summing the corresponding Neumann series, we establish the inequality for the off-diagonal entries (3.10). The proof of Theorem 3.3 is thus complete.

## C Proofs of results in Section 5

In this appendix, we provide the full proof for Theorem 5.1.

### C.1 Proof of Theorem 5.1

From Theorem 2.2 and Theorem 2.4, it follows that for any  $k \neq k'$ , the off-diagonal entries of  $\partial T_N$  satisfy

$$|\partial L_N(k, k')| \leq \exp \{ -|k - k'|^s \}.$$

Following the operator identity in (5.1), we expand each entry  $\partial L_N^{-1}(k, k')$  as a double sum as:

$$\partial L_N^{-1}(k, k') = - \sum_{k_1 \in \Lambda_N} \sum_{k_2 \in \Lambda_N} L_N^{-1}(k, k_1) \partial L_N(k_1, k_2) L_N^{-1}(k_2, k')$$

By applying the triangle inequality and substituting the bounds from Theorem B.1, we obtain:

$$\begin{aligned} |\partial L_N^{-1}(k, k')| &\leq \sum_{k_1 \in \Lambda_N} \sum_{k_2 \in \Lambda_N} |L_N^{-1}(k, k_1)| \cdot |\partial L_N(k_1, k_2)| \cdot |L_N^{-1}(k_2, k')| \\ &\leq \frac{4N^2(2N+1)^{2m}}{\varepsilon_N^2} \left( \exp \left\{ -\frac{\left(|k-k'| - 2N^{\frac{1}{2}}\right)^s}{2} \right\} \right). \end{aligned}$$

Given that the spatial separation satisfies  $|k - k'| \geq N^{\frac{3}{4}}$ , the off-diagonal entries of  $\partial L_N^{-1}$  satisfy the Gevrey bound (5.3). The proof thus is complete.